Published in final edited form as:
Biol Cybern. 2010 July ; 103(1): 57–77. doi:10.1007/s00422-010-0385-7.

Maximizing contrast resolution in the outer retina of mammals

Mikhail Y. Lipin,
Department of Neuroscience, University of Pennsylvania, 123 Anatomy/Chemistry Building, Philadelphia, PA 19104-6058, USA misha@retina.anatomy.upenn.edu; mishalipin@gmail.com

Robert G. Smith, and
Department of Neuroscience, University of Pennsylvania, 123 Anatomy/Chemistry Building, Philadelphia, PA 19104-6058, USA

W. Rowland Taylor
Department of Ophthalmology, Casey Eye Institute, Oregon Health & Science University, Portland, OR 97239, USA

Abstract

The outer retina removes the first-order correlation, the background light level, and thus more efficiently transmits contrast. This removal is accomplished by negative feedback from horizontal cell to photoreceptors. However, the optimal feedback gain to maximize the contrast sensitivity and spatial resolution is not known. The objective of this study was to determine, from the known structure of the outer retina, the synaptic gains that optimize the response to spatial and temporal contrast within natural images. We modeled the outer retina as a continuous 2D extension of the discrete 1D model of Yagi et al. (Proc Int Joint Conf Neural Netw 1: 787–789, 1989). We determined the spatio-temporal impulse response of the model using small-signal analysis, assuming that the stimulus did not perturb the resting state of the feedback system. In order to maximize the efficiency of the feedback system, we derived the relationships between time constants, space constants, and synaptic gains that give the fastest temporal adaptation and the highest spatial resolution of the photoreceptor input to bipolar cells. We found that feedback which directly modulated photoreceptor calcium channel activation, as opposed to changing photoreceptor voltage, provides faster adaptation to light onset and higher spatial resolution. The optimal solution suggests that the feedback gain from horizontal cells to photoreceptors should be ~0.5. The model can be extended to retinas that have two or more horizontal cell networks with different space constants. The theoretical predictions closely match experimental observations of outer retinal function.

Keywords

Lateral inhibition; Feedback; Horizontal cell; Network; Gain

1 Introduction

If, as Barlow (1953) suggested, “the retina is acting as a filter rejecting unwanted information and passing useful information,” then the biophysical mechanisms that underlie early visual processing must tune the retina for high sensitivity to salient information. This raises the question: what information is useful, and how does the retina reject unwanted information?

Correspondence to: Mikhail Y. Lipin.

The work was presented at ARVO, April 2008, Fort Lauderdale, FL.

Since the retina has evolved to resolve natural scenes, it is widely thought that the distribution of contrast within natural scenes will best represent the incoming information that is most salient. As Van Hateren noted (1993), a natural scene consists of simple light contrasts, and its power spectrum is similar to that of an edge (Field 1987). Our perceptual experience nicely illustrates the visual system's sensitivity to contrast edges; we can easily see slight differences in intensity at a sharp boundary, but have difficulty in accurately resolving slight differences in intensity at distant locations (Fig. 1).

It is widely accepted that the outer retina removes the first-order correlation—the background (Barlow 1961; Srinivasan et al. 1982; Tranchina 2002; Yagi et al. 1997). This is the most general function for the first stage of the visual system. Such generality makes sense because there are many ganglion cell types that respond to particular features within a natural image, and all these cell types get input from the outer retina. This implies that the outer retina must serve a more general function than extraction of a particular feature of natural images.

The classical receptive field surround of ganglion cells is formed at least partly in the outer retina (Vigh and Witkovsky 1999; McMahon et al. 2004; Ichinose and Lukasiewicz 2005). The classic Rodieck model (1965) of the receptive field of a ganglion cell as a product of spatial and temporal components matched experimental data well, except that it predicted a small response to full-field light onset, which is not consistent with experiment (Ratliff et al. 1967; Frishman et al. 1987). Dawis et al. (1984) found that spatial and temporal responses are inseparable, and that temporal frequency affects the ratio between the strength of center and surround, the relative phase of center and surround, and the spatial extent of the surround. Empirical models of the ganglion cell receptive field that included a delay in antagonistic surround and several other parameters that provided a good fit to experimental data (Enroth-Cugell and Robson 1966; Frishman et al. 1987).

Few theoretical approaches have been proposed to explain why the retina should have center–surround antagonism. Barlow (1961) proposed the subtraction of surround from center as a mechanism to reduce redundancy and the range of intensity that neurons need to encode. Srinivasan et al. (1982) extended Barlow's idea by introducing noise in downstream circuitry. A reduction in range allows neurons to operate with a higher sensitivity so that the information contained within small signals is less likely to be masked by the intrinsic noise added downstream. Atick and Redlich (1990) maximized the mutual information between retinal input and output, assuming that the goal of visual processing is to recode the sensory data in order to reduce redundancy. Although there is little evidence for the reconstruction of images in the brain, their theory predicted center–surround receptive fields at high signal-to-noise ratios, and agreed with Barlow's hypothesis in the limit of no noise.

Here, we focus on the mechanisms of center surround antagonism in the outer retina. Although much is known about the structure and synaptic function of the outer retina, little is known about the optimal biophysical parameters required to generate center–surround antagonism. Predictive coding and information theories predicted strong dependence of the surround receptive field profile on signal-to-noise ratio, without addressing the biophysical implementation of the center–surround antagonism (Srinivasan et al. 1982; Atick and Redlich 1990). Yagi et al. (1997) developed a biophysical model of the outer retina, but considered optimization of retinal properties an ill-posed problem. In order to show some of the compromises inherent in the design of the outer retina, they used regularization theory (Poggio et al. 1985), which trades accuracy for smoothness. However, their analysis did not find a unique, optimal combination of the outer retina's synaptic gains, space constants, and time constants.

Here, we present a biophysical model for the center–surround receptive field based on the known structure of the outer retina, and consider optimization as a well-posed problem in which a unique solution exists and depends continuously on the retinal properties. Negative feedback reduces the amplitude of the response, and it also tends to reduce the spatial and temporal extent of the center (Smith 1995). Given spatial and temporal constants for horizontal cell and photoreceptor networks, at arbitrary background intensity, we calculated the synaptic gains that simultaneously optimize the amplitude of the response and its spatial and temporal resolution in response to a small change in contrast.

The solution we obtained conforms to experimental data, i.e., the outer retina has a center–surround receptive field, a high sensitivity to a full-field light flash, and the spatial and temporal responses are inseparable. Recently it was shown that the signal-to-noise ratio for the visual system is limited by the outer retina because it loses a factor of approximately fourfold in discriminability (Borghuis et al. 2009). Thus, maximizing the contrast response of the outer retina is critical for visual perception.

2 Methods

2.1 Design problem

Given the known structure of the outer retina and the spatial and temporal constants of photoreceptors and horizontal cells, we optimized synaptic gains to produce the highest spatial and temporal contrast resolution. In order to justify optimizing both spatial and temporal aspects, we note that the background exists as both spatial and temporal correlations, and its removal by negative feedback will affect both spatial and temporal resolutions. As a visual stimulus, we used a white light edge that is an elementary component of natural images. We gave the photoreceptors in the model equal spectral sensitivities to a white light. In order to optimize spatial contrast resolution, we set the visual stimulus to be a small saccade over the light edge, which is equivalent to a light line onset. Large fast eye movement over the light edge, such as a left-to-right saccade between the middle points of the adjacent bars in Fig. 1, is equivalent to a full-field light onset. Thus, we used full-field light onset to optimize temporal contrast resolution.

We defined temporal contrast resolution in the time and frequency domains. In the time domain, removal of the first order correlation in response to full-field light onset occurs when the negative feedback from horizontal cells restores the glutamate release from photoreceptors to near prestimulus levels. The faster the recovery (slew rate) the higher the efficiency of the negative feedback. In the frequency domain, measured neural contrast sensitivity functions reveal an inverse relation between amplitude of response and frequency (Kelly 1971); high frequencies produce lower amplitude responses. A similar relationship applies to the spatial frequency domain (Campbell and Green 1965; Kelly 1973; Michael et al. 2009). Maximizing amplitude is equivalent to maximizing signal-to-noise ratio, and the least spatial and temporal extent of the response gives the highest spatial and temporal resolution. Both of these are necessary to optimize performance for a typical visual scene that contains a mixture of spatial and temporal frequencies many of which are of low contrast. We implemented this trade-off as a multiplication of the magnitude of response times the temporal frequency of the stimulus, which defines the temporal slew rate, or “contrast resolution.” In a similar way, we maximized the spatial contrast resolution. In terms of the impulse response, therefore, the temporal contrast resolution is proportional to the rate of removal of the background (slew rate) in response to full-field light onset, and the spatial contrast resolution is inversely proportional to the spatial extent of the response to a light line onset.

2.2 Model of the outer retina

We assumed "small signal analysis," meaning that the stimulus contrast was low enough to consider the response as linear (Tranchina 2002). Detecting low-contrast images is an evolutionary advantage. Because regions of low contrast are a recurring part of natural images and represent the lower limit to detection, we focused on low contrast images and small signal analysis. The only limitation of the model for high contrasts is a low accuracy due to non-linearities. The mathematical formulation of the outer retina was developed as a continuous 2D extension of the discrete 1D model of Yagi et al. (1989) (Fig. 2). Electrically coupled photoreceptors (Copenhagen and Owen 1976; Lamb and Simon 1976; Detwiler and Hodgkin 1979; DeVries et al. 2002) form a continuous 2D layer (Fig. 2b). The space and time constants of the photoreceptors were defined by longitudinal conductance $g_{p,l}$, membrane conductance $g_{p,m}$, and membrane capacitance c_p. The membrane conductance consists of many components, including non-specific non-gated channels, and ion-selected gated channels, which for practical purposes, can be considered as an average phenomenological or equivalent impedance (Tranchina 2002). Similarly, electrically coupled horizontal cells (Kaneko 1971; Byzov 1975) form a continuous 2D layer (Lankheet et al. 1990), and the space and time constants of this layer were defined by longitudinal conductance $g_{h,l}$, membrane conductance $g_{h,m}$, and membrane capacitance c_h. We included two types of negative feedback from horizontal cells: GABA-ergic feedback, and calcium channel feedback.

Stimulation of photoreceptors by an increase in light intensity, ΔL, results in the following chain of events (Kaneko and Shimazaki 1976; Fesenko et al. 1985): a decrease in cationic membrane conductance $\Delta g_{p,cat}$, a decrease in the cationic current $\Delta I_{p,cat}$, a hyperpolarization of photoreceptors ΔV_p, a decrease in glutamate release ΔGlu, and a hyperpolarization of horizontal cells ΔV_h. The hyperpolarization of horizontal cells ΔV_h decreases feedback current $\Delta I_{p,fb}$ in photoreceptors, and increases the voltage-activated calcium conductance in photoreceptors $\Delta g_{p,Ca}$. The mechanism for the increase is still controversial, but it is generally agreed that the calcium conductance increases due to a shift in the activation range of the voltage-gated calcium channels (Verweij et al. 1996; Babai and Thoreson 2009). In some vertebrates, hyperpolarization of horizontal cells also decreases GABA release that decreases GABA-gated chloride current in horizontal cells $\Delta I_{h,Cl}$ (Stockton and Slaughter 1991; Miller and Dacheux 1983; Kamermans and Werblin 1992). The temporal filtering from phototransduction was omitted to simplify the derivations because it is not much affected by GABA-ergic negative feedback. The effect of this low-pass filtering is roughly equivalent to increasing the photoreceptor time constant (see Sect. 3).

2.3 Mathematical formulation of the outer retina

We consider the responses of photoreceptors and horizontal cells to a small change in light intensity that induces small deviations from the steady-state. Our small signal analysis assumes linearity for small changes (Tranchina 2002). Regardless of static or time-dependent non-linearities due to cooperativity, saturation, voltage-gated channels etc, a small change in membrane potential results in a small change in release/uptake balance that leads to a small change in glutamate concentration. The glutamate release curve is continuous and, therefore, can be approximated as linear over a small range (Rieke and Schwartz 1996), as is diffusion, and binding and unbinding from postsynaptic receptor. Moreover, the rate of glutamate release is thought to be linearly dependent on calcium concentration (Thoreson et al. 2004). The output from the outer retina, which comprises the input to bipolar cells, is considered to be the glutamate release from the photoreceptors. The change in glutamate-modulated conductance at the ON and OFF bipolar cell dendritic tips is directly proportional to the change in glutamate release.

For large signals, not restricted to the linear range, glutamate release from photoreceptors depends on calcium influx, which is equal to the product of the calcium conductance $g_{p,Ca}$ and the difference between the calcium reversal potential and the photoreceptor membrane potential. For small signals within the linear range, the change in glutamate release is obtained from the partial derivatives (gains) with respect to the variables of interest. Thus, the change in glutamate release, ΔGlu, is the sum of the photoreceptor voltage-induced change and the calcium conductance-induced change. The photoreceptor voltage-induced change is the product of photoreceptor voltage-driven glutamate release gain $\partial Glu/\partial V_p$, and change in photoreceptor voltage, ΔV_p. The calcium conductance-induced change is the product of calcium conductance-driven glutamate release gain $\partial Glu/\partial g_{p,Ca}$ and the change in calcium conductance, $\Delta g_{p,Ca}$:

$$\Delta Glu = \frac{\partial Glu}{\partial V_p}\Delta V_p + \frac{\partial Glu}{\partial g_{p,Ca}}\Delta g_{p,Ca}. \tag{1.1}$$

Similarly, the change in calcium conductance, $\Delta g_{p,Ca}$, is the sum of the photoreceptor voltage-induced change and the horizontal cell voltage-induced change:

$$\Delta g_{p,Ca} = \frac{\partial g_{p,Ca}}{\partial V_p}\Delta V_p + \frac{\partial g_{p,Ca}}{\partial V_h}\Delta V_h. \tag{1.2}$$

The glutamate release is determined mostly by the change in calcium conductance, because the calcium driving force (calcium reversal potential minus photoreceptor membrane potential) does not change much, and therefore the first term in the right side of Eq. 1.1 is insignificant. For example, for a photoreceptor resting potential of −40mV, cytoplasmic calcium concentration is ~3μM, and the calcium reversal potential is about +78mV. Because the calcium current decrease is e-fold for ~4.5mV hyperpolarization (Rieke and Schwartz 1996), the increase in glutamate release due to an increase in calcium driving force is less than 4% of the decrease produced by a change in calcium conductance.

To simplify the model equations below (3.1–3.4), we utilized the following identities:

Space constant of photoreceptors:

$$R_p = \sqrt{\frac{g_{p,l}}{g_{p,m}}}. \tag{2.1}$$

Space constant of horizontal cells:

$$R_h = \sqrt{\frac{g_{h,l}}{g_{h,m}}}. \tag{2.2}$$

Time constant of photoreceptors:

$$T_p = \frac{c_p}{g_{p,m}}. \tag{2.3}$$

Time constant of horizontal cells:

$$T_{\mathrm{h}}=\frac{c_{\mathrm{h}}}{g_{\mathrm{h,m}}}. \tag{2.4}$$

The light sensitivity of photoreceptors is the product of the membrane resistance $1/g_{\mathrm{p,m}}$, the cationic conductance-driven cationic current gain $\partial I_{\mathrm{p,cat}}/\partial g_{\mathrm{p,cat}}$, and the light-driven cationic conductance gain $\partial g_{\mathrm{p,cat}}/\partial L$:

$$S=-\frac{1}{g_{\mathrm{p,m}}}\cdot\frac{\partial I_{\mathrm{p,cat}}}{\partial g_{\mathrm{p,cat}}}\frac{\partial g_{\mathrm{p,cat}}}{\partial L}. \tag{2.5}$$

The feedforward gain from photoreceptors to horizontal cells PH is the product of the membrane resistance $1/g_{\mathrm{h,m}}$, the cationic conductance-driven current gain $\partial I_{\mathrm{h,cat}}/\partial g_{\mathrm{h,cat}}$, glutamate-driven cationic conductance gain $\partial g_{\mathrm{h,cat}}/\partial \mathrm{Glu}$, and the sum of photoreceptor voltage-driven glutamate release gain $\partial \mathrm{Glu}/\partial V_{\mathrm{p}}$ and the product of calcium conductance-driven glutamate release gain $\partial \mathrm{Glu}/\partial g_{\mathrm{p,Ca}}$ and photoreceptor voltage-driven calcium conductance gain $\partial g_{\mathrm{p,ca}}/\partial V_{\mathrm{p}}$:

$$\mathrm{PH}=\frac{1}{g_{\mathrm{h,m}}}\cdot\frac{\partial I_{\mathrm{h,cat}}}{\partial g_{\mathrm{h,cat}}}\frac{\partial g_{\mathrm{h,cat}}}{\partial \mathrm{Glu}}\times\left(\frac{\partial \mathrm{Glu}}{\partial V_{p}}+\frac{\partial \mathrm{Glu}}{\partial g_{\mathrm{p,Ca}}}\frac{\partial g_{\mathrm{p,Ca}}}{\partial V_{\mathrm{p}}}\right). \tag{2.6}$$

The feedback gain from horizontal cells to photoreceptors HP is the product of the photoreceptor-membrane resistance $1/g_{\mathrm{p,m}}$ and the horizontal-voltage-driven feedback current gain $\partial I_{\mathrm{p,fb}}/\partial V_{\mathrm{h}}$:

$$\mathrm{HP}=-\frac{1}{g_{\mathrm{p,m}}}\cdot\frac{\partial I_{\mathrm{p,fb}}}{\partial V_{\mathrm{h}}} \tag{2.7}$$

(HP > 0 for negative feedback).

The feedback loop gain from horizontal cells to photoreceptor calcium channels HCa is the product of the horizontal cell membrane resistance $1/g_{\mathrm{h,m}}$, the horizontal cell cationic conductance-driven current gain $\partial I_{\mathrm{h,cat}}/\partial g_{\mathrm{h,cat}}$, the glutamate-driven horizontal cell cationic conductance gain $\partial g_{\mathrm{h,cat}}/\partial \mathrm{Glu}$, the photoreceptor calcium channel conductance-driven glutamate release gain $\partial \mathrm{Glu}/\partial g_{\mathrm{p,Ca}}$, and the horizontal cell voltage-driven calcium conductance gain $\partial g_{\mathrm{p,ca}}/\partial V_{\mathrm{h}}$:

$$\mathrm{HCa}=-\frac{1}{g_{\mathrm{h,m}}}\cdot\frac{\partial I_{\mathrm{h,cat}}}{\partial g_{\mathrm{h,cat}}}\frac{\partial g_{\mathrm{h,cat}}}{\partial \mathrm{Glu}}\frac{\partial \mathrm{Glu}}{\partial g_{\mathrm{p,Ca}}}\frac{\partial g_{\mathrm{p,Ca}}}{\partial V_{\mathrm{h}}} \tag{2.8}$$

(HCa > 0 for negative feedback).

The feedback loop gain from horizontal cells to themselves via $\mathrm{GABA_A}$ receptors HG is the product of the horizontal cell membrane resistance $1/g_{\mathrm{h,m}}$, the GABA-driven chloride current gain $\partial I_{\mathrm{h,Cl}}/\partial \mathrm{GABA}$, and the horizontal cell voltage-driven GABA release gain $\partial \mathrm{GABA}/\partial V_{\mathrm{h}}$:

$$\mathrm{HG}=\frac{1}{g_{\mathrm{h,m}}}\frac{\partial I_{\mathrm{h,Cl}}}{\partial \mathrm{GABA}}\frac{\partial \mathrm{GABA}}{\partial V_{\mathrm{h}}} \tag{2.9}$$

(HG > 0 for positive feedback).

The glutamate released induces an autofeedback current in photoreceptors through a negative feedback mechanism (Picaud et al. 1995; Hosoi et al. 2005) or via glutamate transporters (Tachibana and Kaneko 1988). Such autofeedback to photoreceptors would affect the photoreceptor membrane conductance, which would in turn affect the photoreceptor time constant, photoreceptor sensitivity, and horizontal cell voltage feedback gain. Since the conclusions from the model were essentially the same with or without autofeedback, we omitted autofeedback here to simplify the equations.

For the above parameter definitions (2.1– 2.10) and assuming small signal analysis, the decrements of membrane potentials of photoreceptors $\mathrm{d}V_{\mathrm{p}}$ and horizontal cells $\mathrm{d}V_{\mathrm{h}}$ in the range from r to $r + \mathrm{d}r$ (Fig. 2b) are equal to the ratios of longitudinal current to longitudinal conductance (Ohm's law):

$$-\mathrm{d}V_{\mathrm{p}}=I_{\mathrm{p,l}}\frac{\mathrm{d}r}{2\pi r g_{\mathrm{p,l}}}, \tag{3.1}$$

$$-\mathrm{d}V_{\mathrm{h}}=I_{\mathrm{h,l}}\frac{\mathrm{d}r}{2\pi r g_{\mathrm{h,l}}}. \tag{3.2}$$

The decrement of the longitudinal current in the photoreceptor layer is equal to the sum of membrane leakage current, capacitive current, horizontal cell feedback current, and phototransduction current:

$$-\mathrm{d}I_{\mathrm{p,l}}=g_{\mathrm{p,m}}2\pi\, r\,\mathrm{d}r\left(\Delta V_{\mathrm{p}}+T_{\mathrm{p}}\frac{\mathrm{d}V_{\mathrm{p}}}{\mathrm{d}t}+\mathrm{HP}\cdot\Delta V_{\mathrm{h}}+S\cdot\Delta L\right). \tag{3.3}$$

The decrement of the longitudinal current in the horizontal cell layer is equal to the sum of the membrane leakage current, capacitive current, calcium channel feedback current, minus the GABA-ergic auto-feedback current and glutamatergic input from photoreceptors:

$$-\mathrm{d}I_{\mathrm{h,l}}=g_{\mathrm{h,m}}2\pi\, r\,\mathrm{d}r\left(\Delta V_{\mathrm{h}}+T_{\mathrm{h}}\frac{\mathrm{d}V_{\mathrm{h}}}{\mathrm{d}t}+\mathrm{HCa}\cdot\Delta V_{\mathrm{h}}-\mathrm{HG}\cdot\Delta V_{\mathrm{h}}-\mathrm{PH}\cdot\Delta V_{\mathrm{p}}\right). \tag{3.4}$$

Substituting the currents $I_{\mathrm{p,l}}$ in (3.3) from (3.1) and $I_{\mathrm{h,l}}$ in (3.4) from (3.2) results in:

$$\begin{cases} R_{\mathrm{p}}^2\frac{1}{r}\frac{\mathrm{d}}{\mathrm{d}r}\left(r\frac{\mathrm{d}}{\mathrm{d}r}\right)V_{\mathrm{p}}-\Delta V_{\mathrm{p}}-T_{\mathrm{p}}\frac{\mathrm{d}V_{\mathrm{p}}}{\mathrm{d}t}-S\cdot\Delta L \\ \quad -\mathrm{HP}\cdot\Delta V_{\mathrm{h}}=0 \\ R_{\mathrm{h}}^2\frac{1}{r}\frac{\mathrm{d}}{\mathrm{d}r}\left(r\frac{\mathrm{d}}{\mathrm{d}r}\right)V_{\mathrm{h}}-(1+\mathrm{HCa}-\mathrm{HG})\cdot\Delta V_{\mathrm{h}}-T_{\mathrm{h}}\frac{\mathrm{d}V_{\mathrm{h}}}{\mathrm{d}t} \\ \quad +\mathrm{PH}\cdot\Delta V_{\mathrm{p}}=0. \end{cases} \tag{4.1 4.2}$$

These equations can be modified to derive the response to a 1D stimulus, such as a light boundary or a sine grating moving in the direction orthogonal to isoluminance lines. To do so, the responses of photoreceptors and horizontal cells are derived from Eqs. 4.1–4.2 by replacing the cylindrical Laplacian by a Cartesian one:

$$\frac{1}{r}\frac{\mathrm{d}}{\mathrm{d}r}\left(r\frac{\mathrm{d}}{\mathrm{d}r}\right)\rightarrow\frac{\mathrm{d}^2}{\mathrm{d}r^2}. \tag{5}$$

2.4 Boundary conditions: response to a small increase in full-field light

The stationary response of photoreceptors and horizontal cells to a full-field light stimulus is found by zeroing the temporal and spatial derivatives in Eqs. 4.1–4.2. In the absence of feedback (HP and HCa = 0), the photoreceptor response $\Delta V_{\mathrm{p},0}$ is equal to the product of transduction sensitivity S and the increment of light intensity ΔL:

$$\Delta V_{\mathrm{p},0}=-S\cdot\Delta L. \tag{6}$$

The stationary full-field light responses of photoreceptors and horizontal cells, $\Delta V_{\mathrm{p,full\text{-}field}}$ and $\Delta V_{\mathrm{h,full\text{-}field}}$, respectively, in the presence of the negative feedback are found from Eqs. 4.1–4.2, 6:

$$\Delta V_{\mathrm{p,full-field}}=\frac{\Delta V_{\mathrm{p},0}(1+\mathrm{HCa}-\mathrm{HG})}{1+\mathrm{HCa}-\mathrm{HG}+\mathrm{PH}\cdot\mathrm{HP}}, \tag{7}$$

$$\Delta V_{\mathrm{h,full-field}}=\frac{\Delta V_{\mathrm{p},0}\mathrm{PH}}{1+\mathrm{HCa}-\mathrm{HG}+\mathrm{PH}\cdot\mathrm{HP}}. \tag{8}$$

The output of the outer retina is transmitted by bipolar cells, which receive inputs of opposite polarity from photoreceptors and horizontal cells. OFF-bipolar cells are excited by photoreceptors and are thought to be inhibited by GABA release from horizontal cells, whereas ON-bipolar cells are inhibited by photoreceptors and are thought to be excited by GABA release from horizontal cells (Vardi et al. 2000; Duebel et al. 2006). For simplicity, we derived a response of one polarity, which represented the response of both types.

Each bipolar cell collects inputs from many photoreceptors to its dendritic tree, however, for simplicity we consider the input from one photoreceptor. Therefore, bipolar cell response means the local response of an isolated bipolar cell dendrite, where ΔV_{b} is a difference between glutamate-driven input from photoreceptors and GABA-ergic input from horizontal cells:

$$\Delta V_{\mathrm{b}}=\frac{\partial V_{\mathrm{b}}}{\partial\mathrm{Glu}}\Delta\,\mathrm{Glu}-\frac{\partial V_{\mathrm{b}}}{\partial\mathrm{GABA}}\frac{\partial\mathrm{GABA}}{\partial V_{\mathrm{h}}}\Delta V_{\mathrm{h}}. \tag{9}$$

Denoting the efficiency of the conversion of glutamate release from photoreceptors to bipolar cell membrane potential CE as the product of glutamate-driven bipolar cell gain $\partial V_{\mathrm{b}}/\partial\mathrm{Glu}$ and the sum of photoreceptor-voltage-driven glutamate release gain $\partial\mathrm{Glu}/\partial V_{\mathrm{p}}$ and the product of photoreceptor-calcium conductance-driven glutamate release gain $\partial\mathrm{Glu}/\partial g_{\mathrm{p,Ca}}$ and the photoreceptor-voltage-driven calcium conductance gain $\partial g_{\mathrm{p,ca}}/\partial V_{\mathrm{p}}$:

$$\mathrm{CE}=\frac{\partial V_\mathrm{b}}{\partial \mathrm{Glu}}\left(\frac{\partial \mathrm{Glu}}{\partial V_\mathrm{p}}+\frac{\partial \mathrm{Glu}}{\partial g_{\mathrm{p,Ca}}}\frac{\partial g_{\mathrm{p,Ca}}}{\partial V_\mathrm{p}}\right); \tag{10}$$

the glutamate-driven change of bipolar cell membrane potential $\Delta V_{\mathrm{b,Glu}}$ will be:

$$\Delta V_{\mathrm{b,Glu}}=\mathrm{CE}\cdot\left(\Delta V_\mathrm{p}-\frac{\mathrm{HCa}}{\mathrm{PH}}\Delta V_\mathrm{h}\right). \tag{11}$$

Denoting the GABA-ergic voltage gain from horizontal cells to bipolar cells HB as:

$$\mathrm{HB}=\frac{\partial V_\mathrm{b}}{\partial \mathrm{GABA}}\frac{\partial \mathrm{GABA}}{\partial V_\mathrm{h}}; \tag{12}$$

the net light-induced change in the bipolar cell membrane potential will be:

$$\Delta V_\mathrm{b}=\mathrm{CE}\cdot\left(\Delta V_\mathrm{p}-\frac{\mathrm{HCa}}{\mathrm{PH}}\Delta V_\mathrm{h}\right)-\mathrm{HB}\cdot\Delta V_\mathrm{h}. \tag{13}$$

The response of bipolar cells to stationary full-field light, $\Delta V_{\mathrm{b,full\text{-}field}}$:

$$\Delta V_{\mathrm{b,full-field}}=\frac{\Delta V_{\mathrm{p},0}\mathrm{CE}\left(1-\mathrm{HG}-\mathrm{HB}\cdot\frac{\mathrm{PH}}{\mathrm{CE}}\right)}{1+\mathrm{HCa}-\mathrm{HG}+\mathrm{PH}\cdot\mathrm{HP}} \tag{14}$$

is equal to zero when the voltage gain from horizontal cells to bipolar cells is equal to:

$$\mathrm{HB}=\frac{\mathrm{CE}\,(1-\mathrm{HG})}{\mathrm{PH}}. \tag{15}$$

In order to simplify the notation further, we derived the following identities: ratio of squares of space constants:

$$\gamma=\frac{R_\mathrm{p}^2}{R_\mathrm{h}^2}(1+\mathrm{HCa}-\mathrm{HG}); \tag{16.1}$$

ratio of time constants:

$$\theta=\frac{T_\mathrm{p}}{T_\mathrm{h}}(1+\mathrm{HCa}-\mathrm{HG}); \tag{16.2}$$

spatial extent of bipolar cell input:

$$R_b = R_p \cdot \sqrt{\frac{2}{1+\gamma}}; \tag{16.3}$$

temporal extent of bipolar cell input:

$$T_b = \frac{2T_p}{1+\theta}; \tag{16.4}$$

dimensionless space variable:

$$x = \frac{r}{R_b}; \tag{16.5}$$

dimensionless time variable:

$$\tau = \frac{t}{T_b}; \tag{16.6}$$

combined feedback loop gain:

$$LG = 1 + \frac{PH \cdot HP}{1 + HCa - HG}; \tag{16.7}$$

dimensionless parameter:

$$\alpha = \sqrt{\frac{1}{2} - \frac{\sqrt{\gamma \cdot LG}}{1+\gamma}}; \tag{16.8}$$

dimensionless parameter:

$$\beta = \sqrt{1 - \frac{4\theta \cdot LG}{(1+\theta)^2}}. \tag{16.9}$$

2.5 Response to a light onset and light edge

The temporal responses of horizontal cells, photoreceptors, and bipolar cells, $\Delta V_{h,flash}$, $\Delta V_{p,flash}$, and $\Delta V_{b,flash}$, respectively, to a full-field light flash at $t = 0$, were derived from Eqs. 4.1–4.2 by zeroing the spatial derivatives, and conditions (7, 8, 14):

$$\Delta V_{h,flash}(\tau) = \frac{4PH \cdot \theta \cdot \Delta V_{p,0} \sinh(\beta\tau) \exp(-\tau)}{T_b (1 + HCa - HG)(1+\theta)^2 \beta}, \tag{17.1}$$

$$\Delta V_{\mathrm{p,flash}}(\tau)=\frac{2\Delta V_{\mathrm{p},0}\exp(-\tau)}{T_{\mathrm{b}}(1+\theta)}\left[\cosh(\beta\tau)-\frac{\sinh(\beta\tau)}{\beta}\right]+\frac{1+\mathrm{HCa}-\mathrm{HG}}{\mathrm{PH}}\Delta V_{\mathrm{h,flash}}, \tag{17.2}$$

$$\Delta V_{\mathrm{b,flash}}(\tau)=\frac{2\mathrm{CE}\cdot\Delta V_{\mathrm{p},0}\exp(-\tau)}{T_{\mathrm{b}}(1+\theta)}\times\left[\cosh(\beta\tau)-\frac{\sinh(\beta\tau)}{\beta}\right]+\left(\frac{\mathrm{CE}(1-\mathrm{HG})}{\mathrm{PH}}-\mathrm{HB}\right)\cdot\Delta V_{\mathrm{h,flash}}. \tag{17.3}$$

Similarly, the temporal step responses of horizontal cells, photoreceptors, and bipolar cells, $\Delta V_{\mathrm{h,onset}}$, $\Delta V_{\mathrm{p,onset}}$, and $\Delta V_{\mathrm{b,onset}}$, respectively, to a full-field light onset were obtained by integration of the corresponding responses to the flash (17.1–17.3) over time $t > 0$:

$$\Delta V_{\mathrm{h,onset}}(\tau)=\frac{\mathrm{PH}\cdot\Delta V_{\mathrm{p},0}}{(1+\mathrm{HCa}-\mathrm{HG})\,\mathrm{LG}}\times\left[1-\left(\cosh(\beta\tau)+\frac{\sinh(\beta\tau)}{\beta}\right)\exp(-\tau)\right], \tag{18.1}$$

$$\Delta V_{\mathrm{p,onset}}(\tau)=\frac{2\Delta V_{\mathrm{p},0}}{1+\theta}\frac{\sinh(\beta\tau)}{\beta}\exp(-\tau)+\frac{1+\mathrm{HCa}-\mathrm{HG}}{\mathrm{PH}}\Delta V_{\mathrm{h,onset}}, \tag{18.2}$$

$$\Delta V_{\mathrm{b,onset}}(\tau)=\frac{2\mathrm{CE}\cdot\Delta V_{\mathrm{p},0}}{1+\theta}\frac{\sinh(\beta\tau)}{\beta}\exp(-\tau)+\left(\frac{\mathrm{CE}(1-\mathrm{HG})}{\mathrm{PH}}-\mathrm{HB}\right)\cdot\Delta V_{\mathrm{h,onset}}. \tag{18.3}$$

The 1D spatial impulse responses of horizontal cells, photoreceptors, and bipolar cells, $\Delta V_{\mathrm{h,line}}$, $\Delta V_{\mathrm{p,line}}$, and $\Delta V_{\mathrm{b,line}}$, respectively, to a narrow stationary light bar at $r = 0$ were derived from Eqs. 4.1–4.2 by zeroing the temporal derivatives, Cartesian Laplacian (5.2), and conditions (7, 8, 14):

$$\Delta V_{\mathrm{h,line}}(x)=\frac{\mathrm{PH}\cdot\Delta V_{\mathrm{p},0}\sqrt{\gamma}\cdot\exp\left(-|x|\sqrt{1-\alpha^2}\right)}{2R_{\mathrm{b}}(1+\gamma)(1+\mathrm{HCa}-\mathrm{HG})\sqrt{\mathrm{LG}}}\times\left(\frac{\cosh(\alpha|x|)}{\sqrt{1-\alpha^2}}+\frac{\sinh(\alpha|x|)}{\alpha}\right), \tag{19.1}$$

$$\Delta V_{\mathrm{p,line}}(x)=\frac{\Delta V_{\mathrm{p},0}\exp\left(-|x|\sqrt{1-\alpha^2}\right)}{2R_{\mathrm{b}}(1+\gamma)}\times\left[\frac{\cosh(\alpha|x|)}{\sqrt{1-\alpha^2}}-\frac{\sinh(\alpha|x|)}{\alpha}\right]+\frac{1+\mathrm{HCa}-\mathrm{HG}}{\mathrm{PH}}\Delta V_{\mathrm{h,line}}, \tag{19.2}$$

$$\Delta V_{\mathrm{b,line}}(x)=\frac{\mathrm{CE}\cdot\Delta V_{p,0}\exp\left(-|x|\sqrt{1-\alpha^2}\right)}{2R_{\mathrm{b}}(1+\gamma)}\times\left[\frac{\cosh(\alpha|x|)}{\sqrt{1-\alpha^2}}-\frac{\sinh(\alpha|x|)}{\alpha}\right]+\left(\frac{\mathrm{CE}(1-\mathrm{HG})}{\mathrm{PH}}-\mathrm{HB}\right)\cdot\Delta V_{\mathrm{h,line}}. \tag{19.3}$$

The 1D spatial step responses of horizontal cells, photoreceptors, and bipolar cells, $\Delta V_{\mathrm{h,edge}}$, $\Delta V_{\mathrm{p,edge}}$, and $\Delta V_{\mathrm{b,edge}}$, respectively, to a stationary light edge were obtained by integration of the corresponding responses to the narrow bar (19.1–19.3) over area $r > 0$:

$$\Delta V_{\mathrm{h,edge}}(x)=\frac{\Delta V_{\mathrm{h,full-field}}}{2}\times\left\{1+\frac{x}{|x|}\left[1-\left(\frac{\sinh(\alpha|x|)}{2\alpha\sqrt{1-\alpha^2}}+\cosh(\alpha|x|)\right)\times\exp\left(-|x|\sqrt{1-\alpha^2}\right)\right]\right\}, \tag{20.1}$$

$$\Delta V_{\mathrm{p,edge}}(x)=\frac{x}{|x|}\frac{\Delta V_{\mathrm{p,0}}\sinh(\alpha|x|)\exp\left(-|x|\sqrt{1-\alpha^2}\right)}{2\alpha\sqrt{1-\alpha^2}(1+\gamma)}+\frac{1+\mathrm{HCa}-\mathrm{HG}}{\mathrm{PH}}\Delta V_{\mathrm{h,edge}}, \tag{20.2}$$

$$\Delta V_{\mathrm{b,edge}}(x)=\frac{x}{|x|}\frac{\mathrm{CE}\cdot\Delta V_{\mathrm{p,0}}\sinh(\alpha|x|)\exp\left(-|x|\sqrt{1-\alpha^2}\right)}{2\alpha\sqrt{1-\alpha^2}(1+\gamma)}+\left(\frac{\mathrm{CE}(1-\mathrm{HG})}{\mathrm{PH}}-\mathrm{HB}\right)\cdot\Delta V_{\mathrm{h,edge}}. \tag{20.3}$$

3 Results

To optimize the negative feedback loop gains, we picked the calcium influx into photoreceptors because it is the earliest point in the model where feedforward and feedback inputs converge. After photopigment isomerization, the negative feedback from horizontal cells increases the calcium influx into photoreceptors, which in turn increases glutamate release. Thus, the glutamate-driven bipolar cell input (Eqs. 17.3, 18.3, 19.3 and 20.3 at HB = 0) reflects calcium influx and was used for optimization of the negative feedback loop gains from horizontal cells. We set the horizontal cell autofeedback gain HG to unity to null the second term in the right sides of Eqs. 17.3, 18.3, 19.3 and 20.3 that is proportional to the horizontal cell response. Exclusion of this term does not significantly change the results yet greatly simplifies the equations; at high feedback loop gains this term is insignificant anyway. Thus HG = 1 unless specified otherwise. We estimated the influence of the horizontal cell autofeedback gain on the outcome of the model in the end of Sect. 3.

3.1 Maximizing temporal and spatial contrast resolution

Large eye movement over a light edge, such as a left-to-right saccade between the middle points of the adjacent bars in Fig. 1, results in a full-field light onset. Horizontal cell feedback mediates a form of post-receptoral light adaptation. Although the term “light adaptation” is sometimes used to describe non-linear effects of changing a background, we use this term in a more general sense to describe any effect of changing a background, including linear subtraction by horizontal cell feedback. The feedback can rapidly subtract the effects of an increase in illumination. One measure of efficiency is the rate at which this is accomplished. As described in Sect. 2, to maximize contrast resolution implies simultaneously maximizing response amplitude and temporal recovery from a change in background, which is equivalent to optimizing slew rate (amplitude per second). For an intensity increase, the fastest slew rate means maximizing the slope of the descending part of the temporal step response (Fig. 3a), so that the glutamate release is restored to its pre-stimulus rate, ready to respond to the next stimulus, in the shortest possible time. The maximal slope of the step response coincides with the maximal undershoot of temporal impulse (flash) response (Fig. 3b).

We assume that the calcium influx controls the feedforward synaptic gain from photoreceptors to horizontal cells; the feedback maximizes the temporal gradient of cytoplasmic calcium concentration. Thus, the faster the increase in intracellular calcium the higher the efficiency of the negative feedback will be, and the larger the signal for synaptic gain control will be. The largest magnitude of the slope (Fig. 3**a**), which corresponds to the magnitude of the calcium

transient, occurs at time t^* from a light onset, that is found by zeroing the first temporal derivative of the impulse response (Eq. 17.3 at HB = 0):

$$t^* = \frac{2T_b}{\beta} \operatorname{artanh}(\beta). \tag{21}$$

Substituting t^*/T_b for τ in Eq. 18.3, we obtained a dependence of the largest magnitude of the calcium transient on parameter β:

$$\left.\frac{dV_{b,onset}}{dt}\right|_{t=t^*} = -\Delta V_{p,0} \frac{CE}{T_p} \left(\frac{1-\beta}{1+\beta}\right)^{\frac{1}{\beta}}. \tag{22}$$

Horizontal cells are known to feed back to photoreceptors by modulating the calcium channel conductance $g_{p,Ca}$ without changing photoreceptor membrane potential (Verweij et al. 1996; Babai and Thoreson 2009). At zero feedback voltage gain from horizontal cells to photoreceptors (HP = 0), the calcium transient is maximized when β equals zero. Setting β to zero (Eq. 16.9) gives the relationship between the time constants and synaptic gains, which maximizes the increase in glutamate release (calcium transient) in response to a full-field light flash (Fig. 4a):

$$\sqrt{1+HCa-HG+PH \cdot HP} + \sqrt{PH \cdot HP} = \sqrt{\frac{T_h}{T_p}}. \tag{23}$$

However, in some species the feedback voltage gain from horizontal cells to photoreceptors HP was found to be nonzero (Wu 1991). In the case that feed back is mediated exclusively by voltage (HCa = 0, HP > 0), the glutamate release oscillates for large voltage loop gain (Smith 1995).In order to find the maximum of the calcium transient, we analyzed the derivative of the calcium transient with respect to the voltage feedback loop gain. Equation 23 sets the optimal voltage loop gain PH · HP : gains lower than optimal decrease the glutamate release transient, whereas gains greater than optimal cause oscillation of the glutamate release. If the voltage loop gain PH · HP is greater than optimal (Eq. 23) the response to a light flash will oscillate with a period $T_{oscil.}$ (Fig. 4b):

$$T_{oscil.} = T_b \operatorname{Re}\left(\frac{i\pi}{\beta}\right). \tag{24}$$

Thus, the optimal relationship between feedback gains and time constants (Eq. 23) maximizes the slew rate if the only feedback is the calcium channel feedback, and maximizes non-oscillating slew rate at the voltage negative feedback. In terms of frequency response, the slew rate corresponds to the product of the amplitude of response to a sine flicker and the temporal frequency, at which the amplitude is maximal.

The frequency response $F(\omega)$ of the glutamatergic bipolar cell input to full-field sine flicker with light intensity amplitude $\Delta L = \Delta V_{p,0}/S$ and angular frequency ω is derived from Eqs. 4.1, 4.2, 11 by zeroing the spatial derivatives. Because the predominant mechanism of horizontal cell negative feedback in most species is the calcium channel mechanism, we will neglect the voltage feedback mechanism here:

$$|F(\omega)| = \frac{2\mathrm{CE} \cdot \Delta V_{\mathrm{p},0} \cdot \omega T_{\mathrm{h}}}{\sqrt{\left(1+(\omega T_{\mathrm{p}})^2\right)\left((1+\mathrm{HCa}-\mathrm{HG})^2+(\omega T_{\mathrm{h}})^2\right)}}. \tag{25}$$

We found the temporal frequency, ω*, at which the amplitude of response will be maximal, by zeroing the first derivative of the amplitude (25) with respect to ω:

$$\omega^* = \sqrt{\frac{1+\mathrm{HCa}-\mathrm{HG}}{T_{\mathrm{p}} T_{\mathrm{h}}}}. \tag{26}$$

The temporal contrast resolution is the product of the amplitude (25) and the frequency (26):

$$\text{Temporal contrast resolution} = |F(\omega^*)| \cdot \omega^*. \tag{27}$$

We found the feedback loop gain HCa, at which the temporal contrast resolution (27) will be maximal, by zeroing the first derivative of the contrast resolution (27) with respect to HCa :

$$1+\mathrm{HCa}-\mathrm{HG} = \frac{T_{\mathrm{h}}}{T_{\mathrm{p}}}. \tag{28}$$

The relationship (28) maximizes the temporal contrast resolution in terms of frequency response, and corresponds to the relationship (23), which maximizes the contrast resolution in response to light onset at zero voltage feedback gain.

In order to find the relationship between the space constants and synaptic gains, we maximized the calcium transient in response to a small shift over a light edge, which is equivalent to an onset of a light line. The calcium transient is proportional to the transient of the glutamate driven bipolar cell input in response to a light line onset:

$$\begin{aligned} \text{Calcium transient}\,(r,t) &\sim \frac{\mathrm{d}}{\mathrm{d}t}\int_0^t G_{\mathrm{Glu}}(r,\xi)\mathrm{d}\xi \\ &= G_{\mathrm{Glu}}(r,t), \end{aligned} \tag{29}$$

where $G_{\mathrm{Glu}}(r, t)$ is the spatio-temporal impulse response of glutamate release, which is derived from Eqs. 4.1–4.2, 11.

Integrating the calcium transient (29) over total area gives the total calcium transient in response to a light line onset, which is proportional to the glutamate release in response to a full-field light flash (undershoot in Fig. 3b). As we found earlier, the calcium transient in response to full-field flash is maximal at the moment $t = t^*$ (Eq. 21), so the calcium transient in response to the line onset will be maximal at the same moment. The space constants determine the spread of the calcium transient over space. The less the spatial spread of the calcium transient, the larger its local magnitude to overcome synaptic noise. In order to minimize the spread of the calcium transient (29) over space, we maximized the magnitude of its first spatial derivative (Fig. 4a) by zeroing the second spatial derivative of the impulse response $G_{\mathrm{Glu}}(r, t^*)$:

$$\frac{\mathrm{d}^2 G_{\mathrm{Glu}}(r,t^*)}{\mathrm{d}r^2}=0. \tag{30}$$

Solution of the Eq. 30 gives the largest slope of the local calcium transient at $t = t^*$ (Fig. 5a), and is also derived by maximizing the slope of the feedback-induced bipolar cell input in response to a static line (Eq. 19.3).

$$\frac{\mathrm{d}\,V_{\mathrm{b,line}}(x)}{r}=\frac{\mathrm{CE}\cdot\Delta V_{\mathrm{p,0}}\exp\left(-|x|\sqrt{1-\alpha^2}\right)}{2R_{\mathrm{p}}^2}\times\left[\frac{\sinh(\alpha|x|)}{2\alpha\sqrt{1-\alpha^2}}-\cosh(\alpha|x|)\right]. \tag{31}$$

The larger this slope (Fig. 5b), the less the extent of the lateral inhibition, and hence, the higher the bipolar cell's spatial resolution will be. The largest slope occurs at a distance from a light line:

$$r^*=\frac{3R_{\mathrm{b}}}{\alpha}\operatorname{artanh}\left(\frac{\alpha}{\sqrt{1-\alpha^2}}\right). \tag{32}$$

At zero feedback voltage gain from horizontal cells to photoreceptors (Fig. 6a), this slope is maximized by setting parameter α (Eq. 16.8) equal to zero. This gives the relationship between the space constants and the synaptic gains:

$$\sqrt{1+\mathrm{HCa}-\mathrm{HG}+\mathrm{PH}\cdot\mathrm{HP}}+\sqrt{\mathrm{PH}\cdot\mathrm{HP}}=\frac{R_{\mathrm{h}}}{R_{\mathrm{p}}}. \tag{33}$$

In the case of an exclusively voltage feedback (HCa = 0), Eq. 33 maximizes the non-oscillating slope (31). In a similar way to the temporal contrast response, if the voltage loop gain PH · HP is greater than specified by Eq. 33 the slope oscillates with a spatial period $R_{\mathrm{oscil.}}$ (Fig. 6b):

$$R_{\mathrm{oscil.}}=R_{\mathrm{b}}\mathrm{Re}\left(\frac{i\pi}{\alpha}\right). \tag{34}$$

We optimized the negative feedback gains for the maximal spatial contrast resolution using spatial sine grating with the spatial frequency *k*. Similar to the equations for temporal contrast resolution (27), we consider the case of exclusively calcium channel feedback. We derived the frequency response *F*(*k*) of the glutamatergic bipolar cell input from Eq. 4.1, 4.2, 11:

$$F(k)=\frac{2\mathrm{CE}\cdot\Delta V_{\mathrm{p,0}}\cdot k^2R_{\mathrm{h}}^2}{\left(1+k^2R_{\mathrm{p}}^2\right)\left(1+\mathrm{HCa}-\mathrm{HG}+k^2R_{\mathrm{h}}^2\right)}. \tag{35}$$

We found the spatial frequency, *k**, at which the amplitude of response will be maximal by zeroing the first derivative of the amplitude (35) with respect to *k*:

$$k^{*^2}=\frac{\sqrt{1+\mathrm{HCa}-\mathrm{HG}}}{R_{\mathrm{p}}R_{\mathrm{h}}}. \tag{36}$$

Since the retina is not sensitive to static images, we maximized the transient response to a spatial sine grating. In order to produce a transient response, we modulated a spatial grating with temporal frequency ω and amplitude $r_0 \ll 1/k^*$. The time-dependent component is proportional to $k^* r_0 \cdot \sin(\omega t)$. Low temporal frequency modulation ($\omega \ll 1/T_p$) does not change the spatial frequency k^*, but allows the retina to see the spatial sine grating. Thus, the transient component of the spatial contrast resolution will be proportional to the product of amplitude $F(k^*)$ (35) and square of the spatial frequency k^*:

$$\text{Spatial contrast resolution} = F(k^*) \cdot k^{*2}. \tag{37}$$

We found the feedback loop gain HCa, at which the spatial contrast resolution will be maximal, by zeroing the first derivative of the contrast resolution (37) with respect to HCa:

$$1 + \text{HCa} - \text{HG} = \frac{R_h^2}{R_p^2}. \tag{38}$$

Comparison of (23) and (33) gives the equation that relates space and time constants:

$$\frac{R_p^2}{T_p} = \frac{R_h^2}{T_h}. \tag{39}$$

The ratios in Eq. 39 have the same dimension as a diffusion coefficient, and describe the spread of electrical signals along the photoreceptor and horizontal cell layers.

To find responses to a complex spatio-temporal visual stimulus, we need to solve the system of Eqs. (4.1–4.2). This system has a simple analytical solution for the set of relationships between space constants, time constants, and feedback loop gains (23, 33) that maximize the calcium transient.

3.2 Spatio-temporal impulse response

To find the response of horizontal cells, photoreceptors, and bipolar cells to an arbitrary stimulus, we derived their impulse responses from Eqs. 4.1–4.2. In a linear system, the responses of horizontal cells, photoreceptors, and bipolar cells to a complex visual stimulus are found by convolution of the stimulus with their respective impulse responses. This complete model of the outer retina included feedforward excitation of horizontal cell from photoreceptors (PH), both voltage (HP) and calcium channel (HCa) feedback from horizontal cells to photoreceptors, autofeedback to horizontal cells (HG), photoreceptor coupling (x), horizontal cell coupling (x), and feedforward signaling to bipolar cells from horizontal cells (HB) and photoreceptors (CE). The 1D and 2D impulse responses of horizontal cells ($G_{h,1D}$, $G_{h,2D}$), photoreceptors ($G_{p,1D}$, $G_{p,2D}$), and bipolar cell input ($G_{b,1D}$ and $G_{b,2D}$), normalized to $\Delta V_{p,0}$ (6), are derived from Eqs. 4.1–4.2, 13 at conditions (7, 8), and relationships (23), (33):

$$G_{h,1D}(x,\tau) = \frac{\text{PH} \cdot \sqrt{\tau} \cdot \exp\left(-\frac{x^2}{4\tau} - \tau\right)}{R_b T_b 2\sqrt{\pi}\,(1 + \text{HCa} - \text{HG} + \text{PH} \cdot \text{HP})}, \tag{40}$$

$$G_{\mathrm{h,2D}}(x,\tau)=\frac{\mathrm{PH}\cdot\exp\left(-\frac{x^2}{4\tau}-\tau\right)}{R_\mathrm{b}^2T_\mathrm{b}4\pi\,(1+\mathrm{HCa}-\mathrm{HG}+\mathrm{PH}\cdot\mathrm{HP})}, \tag{41}$$

$$G_{\mathrm{p,1D}}(x,\tau)=\frac{(1-\tau)\cdot\exp\left(-\frac{x^2}{4\tau}-\tau\right)}{R_\mathrm{b}T_\mathrm{b}\sqrt{\pi}\,(1+\gamma)\sqrt{\tau}}+\frac{1+\mathrm{HCa}-\mathrm{HG}}{\mathrm{PH}}G_{\mathrm{h,1D}}(x,\tau), \tag{42}$$

$$G_{\mathrm{p,2D}}(x,\tau)=\frac{(1-\tau)\cdot\exp\left(-\frac{x^2}{4\tau}-\tau\right)}{R_\mathrm{b}^2T_\mathrm{b}2\pi\,(1+\gamma)\tau}+\frac{1+\mathrm{HCa}-\mathrm{HG}}{\mathrm{PH}}G_{\mathrm{h,2D}}(x,\tau), \tag{43}$$

$$G_{\mathrm{b,1D}}(x,\tau)=\frac{\mathrm{CE}\cdot(1-\tau)\cdot\exp\left(-\frac{x^2}{4\tau}-\tau\right)}{R_\mathrm{b}T_\mathrm{b}\sqrt{\pi}\,(1+\gamma)\sqrt{\tau}}+\left(\frac{\mathrm{CE}\,(1-\mathrm{HG})}{\mathrm{PH}}-\mathrm{HB}\right)G_{\mathrm{h,1D}}(x,\tau), \tag{44}$$

$$G_{\mathrm{b,2D}}(x,\tau)=\frac{\mathrm{CE}\cdot(1-\tau)\cdot\exp\left(-\frac{x^2}{4\tau}-\tau\right)}{R_\mathrm{b}^2T_\mathrm{b}2\pi\,(1+\gamma)\tau}+\left(\frac{\mathrm{CE}\,(1-\mathrm{HG})}{\mathrm{PH}}-\mathrm{HB}\right)G_{\mathrm{h,2D}}(x,\tau). \tag{45}$$

Note that spatial and temporal variables are not in separate terms in the impulse responses (40–45) because the model is based on a biophysical system where spatial diffusion of a signal changes over time. The spatio-temporal bipolar cell impulse responses above represent the center–surround receptive field when measured with an infinitely small and short stimulus. Below we derive the spatial and temporal impulse responses separately in order to compare the model with commonly obtained experimental data.

3.3 Spatial receptive field of outer retina has center–surround antagonism

In order to find 1D and 2D static spatial impulse responses, we excluded the temporal component by integration of Eqs. 40–45 over time:

$$G_{\mathrm{h,1D}}(x)=\frac{\mathrm{PH}\cdot(1+x)\exp(-x)}{4R_\mathrm{b}\,(1+\mathrm{HCa}-\mathrm{HG}+\mathrm{PH}\cdot\mathrm{HP})}, \tag{46}$$

$$G_{\mathrm{h,2D}}(x)=\frac{\mathrm{PH}\cdot xK_1(x)}{R_\mathrm{b}^2 4\pi\,(1+\mathrm{HCa}-\mathrm{HG}+\mathrm{PH}\cdot\mathrm{HP})}, \tag{47}$$

$$G_{\mathrm{p,1D}}(x)=\frac{(1-x)\exp(-x)}{2R_\mathrm{b}\,(1+\gamma)}+\frac{1+\mathrm{HCa}-\mathrm{HG}}{\mathrm{PH}}G_{\mathrm{h,1D}}(x), \tag{48}$$

$$G_{\mathrm{p,2D}}(x)=\frac{2K_0(x)-xK_1(x)}{R_\mathrm{b}^2 2\pi(1+\gamma)}+\frac{1+\mathrm{HCa}-\mathrm{HG}}{\mathrm{PH}}G_{\mathrm{h,2D}}(x), \tag{49}$$

$$G_{\mathrm{b,1D}}(x)=\frac{\mathrm{CE}\cdot(1-x)\exp(-x)}{2R_\mathrm{b}(1+\gamma)}+\left(\frac{\mathrm{CE}(1-\mathrm{HG})}{\mathrm{PH}}-\mathrm{HB}\right)\cdot G_{\mathrm{h,1D}}(x), \tag{50}$$

$$G_{\mathrm{b,2D}}(x)=\frac{\mathrm{CE}[2K_0(x)-xK_1(x)]}{R_\mathrm{b}^2 2\pi(1+\gamma)}+\left(\frac{\mathrm{CE}(1-\mathrm{HG})}{\mathrm{PH}}-\mathrm{HB}\right)G_{\mathrm{h,2D}}(x), \tag{51}$$

where $K_0(x)$ and $K_1(x)$ are the modified Bessel functions of the second kind:

$$K_0(x)=\int_0^\infty \exp\left(-x\frac{e^y+e^{-y}}{2}\right)\mathrm{d}y,$$
$$K_1(x)=\int_0^\infty \frac{e^y+e^{-y}}{2}\exp\left(-x\frac{e^y+e^{-y}}{2}\right)\mathrm{d}y.$$

Widely used methods to map a receptive field are to present a narrow light slit at various distances from the cell, which gives the 1D spatial impulse response, and to present a spot of increasing diameter, which gives the 2D spatial step response. Therefore, the derived 1D spatial impulse response (46) and the 2D step response (51) are analogous to receptive field maps, and both display center–surround antagonism (Fig. 7).

3.4 Temporal bipolar cell input consists of excitatory and inhibitory time domains

The temporal impulse responses of horizontal cells, photoreceptors, and bipolar cell input, $G_{\mathrm{h,flash}}(\tau)$, $G_{\mathrm{p,flash}}(\tau)$, and $G_{\mathrm{b,flash}}(\tau)$, respectively, to a full-field light flash (Fig. 8), are the integrals of spatio-temporal impulse responses (41, 43, 45) over the total area:

$$G_{\mathrm{h,flash}}(\tau)=\frac{\mathrm{PH}\cdot\tau\exp(-\tau)}{T_\mathrm{b}(1+\mathrm{HCa}-\mathrm{HG}+\mathrm{PH}\cdot\mathrm{HP})}, \tag{52}$$

$$G_{\mathrm{p,flash}}(\tau)=\frac{2(1-\tau)\exp(-\tau)}{T_\mathrm{b}(1+\theta)}+\frac{1+\mathrm{HCa}-\mathrm{HG}}{\mathrm{PH}}G_{\mathrm{h,flash}}(\tau), \tag{53}$$

$$G_{\mathrm{b,flash}}(\tau)=\frac{2\mathrm{CE}\cdot(1-\tau)\exp(-\tau)}{T_\mathrm{b}(1+\theta)}+\left(\frac{\mathrm{CE}(1-\mathrm{HG})}{\mathrm{PH}}-\mathrm{HB}\right)G_{\mathrm{h,flash}}(\tau). \tag{54}$$

Note that spatial and temporal extents of the bipolar cell input, R_b (Eq. 16.3) and T_b (Eq. 16.4), respectively, for calcium channel feedback are less than those for voltage feedback, by a factor of $\sqrt{2}$ and 2, respectively (Fig. 7a, Fig. 8a). The lower the space and time extents, the higher the spatial resolution and the rate of temporal adaptation. On the other hand, low spatial and

temporal extents result in smaller step responses for calcium channel feedback compared to those for voltage feedback (Fig. 7b, Fig. 8b).

In the absence of negative feedback to photoreceptors, the surround antagonism of bipolar cells could be formed by feedforward inhibition from horizontal cells to bipolar cells, and the model produces identical bipolar cell inputs for GABAergic feedforward inhibition and calcium channel feedback. For example, the bipolar cell input in response to a light flash (Eq. 54) will be the same for HB = CE/PH, HG = 0, HCa = 0 (GABAergic feedforward, no feedback) and for HB = 0, HG = 1, HCa = T_h/T_p (calcium channel feedback, no feedforward).

3.5 The bipolar cell input in response to light spot onset

The spatio-temporal response of photoreceptors (Eqs. 42, 43), horizontal cells (Eqs. 40, 41), and bipolar cells (Eqs. 45, 45) is more complex than a product of separate spatial and temporal components. For the onset of spot stimuli, the bigger the spot, the more transient the bipolar cell response will be. The sustained component of the response is maximal for a light spot that fits the receptive field center, but as the spot gets larger, the sustained component approaches zero (Fig. 9).

3.6 Bipolar cell response is band-passed

To calculate the filtering properties of the model, we used a moving sine grating as a stimulus (Packer and Dacey 2002; Linsenmeier et al. 1982; He and Levick 2000), but we reduced it to one dimension as described in Sect. 2. The bipolar cell input $\Delta V_{b,oscil.line}$ in response to a line, which is sinusoidally modulated with amplitude $\Delta V_{p,0}/S$ and angular frequency ω at an offset x from a photoreceptor, is the convolution of the impulse response (45) and the oscillating line:

$$\Delta V_{b,oscil.line}=\frac{CE\cdot\Delta V_{p,0}\exp\left(i\omega t-|x|\sqrt{1+i\omega T_b}\right)}{2R_b\left(1+\gamma\right)}\times\frac{1+2i\omega T_b-|x|\sqrt{1+i\omega T_b}}{\sqrt{\left(1+i\omega T_b\right)^3}}. \tag{55}$$

Integrating Eq. 55 over space gives the bipolar cell input $\Delta V_{b,mov.gr.}$ in response to a sine grating, which is moving with velocity υ = ω/k, where $k = 2\pi/\lambda$ is a spatial frequency, and λ is the spatial period:

$$\Delta V_{b,mov.gr.}=\frac{2CE\cdot\Delta V_{p,0}}{1+\gamma}\times\frac{k^2R_b^2+i\omega T_b}{\left(1+k^2R_b^2+i\omega T_b\right)^2}\exp\left(i\omega t-ikr\right). \tag{56}$$

The amplitude of the response to a moving sine grating (Eq. 56; Fig.10) is maximal at the spatio-temporal frequencies set by the following relationship:

$$\left(\omega T_b\right)^2+\left(k^2R_b^2\right)^2=1. \tag{57}$$

The bipolar cell input in response to a counter-phasing grating $\Delta V_{b,counteph.gr.}$ is the sum of responses to sine gratings moving in the opposite directions:

$$\Delta V_{b,counterph.gr.}=\frac{2CE\cdot\Delta V_{p,0}}{1+\gamma}\frac{k^2R_b^2+i\omega T_b}{\left(1+k^2R_b^2+i\omega T_b\right)^2}\times\cos\left(kr\right)\exp\left(i\omega t\right). \tag{58}$$

This response can be zeroed or maximized by placing the node ($kr = \pi/2$) or antinode ($kr = 0$), respectively, on the photoreceptor.

The response of a horizontal cell $\Delta V_{\mathrm{h,mov.gr.}}$ and photoreceptor $\Delta V_{\mathrm{p,mov.gr.}}$ to a moving sine grating is calculated as a convolution of the grating and the impulse-response of the horizontal cell (Eq. 40) and photoreceptor (Eq. 42), respectively:

$$\Delta V_{\mathrm{h,mov.gr.}} = \frac{\mathrm{PH} \cdot \Delta V_{\mathrm{p},0}}{1 + \mathrm{HCa} - \mathrm{HG} + \mathrm{PH} \cdot \mathrm{HP}} \times \frac{\exp(i\omega t - ikr)}{(1 + k^2 R_{\mathrm{b}}^2 + i\omega T_{\mathrm{b}})^2}, \tag{59}$$

$$\Delta V_{\mathrm{p,mov.gr.}} = \frac{2\Delta V_{\mathrm{p},0} \exp(i\omega t - ikr)}{1+\gamma} \times \frac{k^2 R_{\mathrm{b}}^2 + i\omega T_{\mathrm{b}}}{(1 + k^2 R_{\mathrm{b}}^2 + i\omega T_{\mathrm{b}})^2} + \frac{1 + \mathrm{HCa} - \mathrm{HG}}{\mathrm{PH}} \Delta V_{\mathrm{h,mov.gr.}}. \tag{60}$$

3.7 Receptive field sizes of bipolar cells and horizontal cells depend on feedback loop gains

The model derived the bipolar and horizontal cell receptive fields as differences of wide and narrow exponentials (Eqs. 19.1 and 19.3; Fig.11). The negative feedback suppresses the spread of membrane potential change along the photoreceptor and horizontal cell networks. Therefore, the feedback reduces the amplitude and width of the bipolar receptive field center (overshoot in Fig. 5b; Smith 1995). In the absence of negative feedback and horizontal cell autofeedback, the large space constant is equal to the horizontal cell space constant R_{h} (Eq. 2.2), whereas the small space constant is equal to the photoreceptor space constant R_{p} (Eq. 2.1). In a discrete network, a second space constant could originate from finite size of horizontal cells (Packer and Dacey 2002; Van Hateren 2007). As the feedback loop gain is increased, the wider exponential narrows. On the other hand, the gain of the horizontal cell autofeedback HG directly subtracts from the negative feedback gain HCa (Eqs. 19.1, 19.3), expanding the wider exponential (see Kamermans and Werblin 1992). Finally, at the optimal feedback loop gain (Eq. 33) the wide and narrow exponentials become close in width.

3.8 Effect of temporal filtering in the outer segments of photoreceptors

In the model, we neglected temporal filtering of the light response in the outer segments of photoreceptors. In real retinas, the impulse response of cones, is thought to be fast (~20 ms) and monophasic (Friedburg et al. 2004; Van Hateren and Lamb 2006). In order to estimate the effect of temporal filtering in the outer segments, we took the cone impulse response (Fig. 9 from Friedburg et al. 2004 at low flash intensity of 22 Td·s), and convolved it with the impulse response of the model's bipolar cell input (Eq. 17.3). As shown in Fig. 12, the duration of the convolved impulse response is determined mostly by the temporal filtering in the outer segments. The effect of the temporal filtering can be taken into account in the model by adding the rise time of the low-pass filter in the outer segments to the time constant of the photoreceptors. As a result, the increase in duration of the photoreceptor impulse response would require less feedback to match the horizontal cell time constant.

Thus, the low-pass filtering in the outer segments (OS) reduces the feedback loop gain required for the maximal temporal contrast resolution (Eq. 23). A real retina with a horizontal cell time constant of ~65 ms Kamermans and Werblin 1992), and a cone time constant of ~5 ms without the OS low-pass filter (Smith and Lamb 1997;Nikonov et al. 2006) would require an optimal feedback loop gain of ~13. However, the OS low-pass filter rise time of ~7–8 ms (Friedburg et al. 2004) will increase the effective cone time constant to 12–13 ms, thus reducing the

predicted optimal feedback loop gain to ~5, closer to the value of ~5.3 in real retinas (estimated from Verweij et al. 1996;Rieke and Schwartz 1996).

3.9 Sensitivity of the model to the horizontal cell autofeedback gain

To derive the optimal relationships between spatio-temporal constants and synaptic gains (Eqs. 23 and 33), we set the horizontal cell autofeedback gain HG to unity, which simplified the equations. This was justified because the horizontal cell positive autofeedback is strong enough to affect significantly the horizontal cell response (Kamermans and Werblin 1992). Furthermore, the membrane potential of horizontal cells tends to oscillate under the block of the negative feedback by HEPES (Normann and Pochobradský 1976) implying an autofeedback gain of ~1. Nevertheless, to allow for arbitrary HG, using the equations which were derived at HG = 1, we must estimate the sensitivity of the results to the autofeedback gain.

As shown in Fig. 13, as the magnitude of the horizontal cell autofeedback gain increases so does the feedback-induced slew rate in response to full-field light onset (calculated using Eq. 17.3 derived at arbitrary HG). The slew rate changes by ~40% of the change in the autofeedback gain. In order to estimate the errors in these calculations, associated with using the simplified equations derived with HG = 1 (Eqs. 40–54), we plotted the calculating error as a function of HG (Fig. 13). One can see that the calculating error is less than 1% in the range of HG from 0 (no autofeedback) to 2, demonstrating that the simplified equations produce accurate results over a wide range of horizontal cell autofeedback gains.

3.10 Sensitivity of the model to feedback gain

The magnitude of the slew rate depends on feedback loop gains, which are the product of the feedforward and feedback gains. The magnitude of the slew rate is not very sensitive to this product. For the calcium channel feedback, a two-fold increase or decrease in feedback loop gain would decrease the slew rate of bipolar cell input by ~8% (from Eq. 17.3). Ten-fold increase or decrease in feedback gain would decrease the slew rate by one half (Figs. 4a, 6a, 14).

The calcium channel feedback loop gain can be estimated from the data of Verweij et al. (1996), which shows that horizontal cells shift the activation range of photoreceptor calcium channels by 7.5 mV. Assuming that the calcium current increases e-fold per 4.5 mV depolarization (Rieke and Schwartz 1996) the calcium channel feedback loop gain HCa will be about exp(7.5/4.5) ≈ 5.3. From this loop gain and photoreceptor-horizontal cell feedforward gain ~10 (Wu 1991), the calcium channel feedback gain can be estimated as HCa/PH ≈ 0.5. As we demonstrate below, the feedback gain estimate (~0.5) is not just the empirical value, but this is optimized to match the magnitudes of photoreceptor and horizontal cell responses:

$$\left|\frac{\Delta V_{\mathrm{p,mov.gr.}}}{\Delta V_{\mathrm{h,mov.gr.}}}\right| = \frac{2\,(1+\mathrm{HCa}-\mathrm{HG}+\mathrm{PH}\cdot\mathrm{HP})}{\mathrm{PH}\,(1+\gamma)} + \frac{1+\mathrm{HCa}-\mathrm{HG}}{\mathrm{PH}}. \tag{61}$$

In the case of exclusively calcium channel feedback (HP = 0), this ratio is unity at calcium feedback gain HCa equal to 0.5 times the feedforward gain from photoreceptors to horizontal cells PH. Calcium channel feedback loop gain is a product of feedforward gain PH and feedback gain on calcium channels, i.e., calcium channel feedback gain HCa/PH is equal to 0.5:

$$\frac{\mathrm{HCa}}{\mathrm{PH}} = 0.5. \tag{62}$$

In the case of exclusively voltage feedback (HCa = 0), this ratio is unity when the voltage feedback gain from horizontal cells to photoreceptors equals 0.5:

$$\mathrm{HP}=0.5. \tag{63}$$

This is similar to the value of 0.3 found in salamander retina (Wu 1991). Thus, regardless of the mechanism of the feedback from horizontal cells to photoreceptors, to equalize the magnitudes of photoreceptor and horizontal cell responses the feedback gain should be about 0.5.

3.11 Extension of the model for two horizontal cell networks

The model can be extended to retinas that have two horizontal cell networks with different space constants. Let V_{h1}^{*} be a membrane potential of a horizontal cell with space constant R_{h1} and feedforward gain PH_1^{*} in the outer retina with a single horizontal cell network. Adding the second horizontal cell network with space constant R_{h2} to Eqs. 4.1–4.2 would not affect the solution for glutamate release if the feedback loop gains are matched to the network space constant (Eq. 33). In this case, two networks act as one with membrane potential V_{h1}^{*} equal to sum of the voltages on each network V_{h1} and V_{h2}, and feedforward gain PH_1^{*} equal to weighted sum of network feedforward gains PH_1 and PH_2:

$$V_{\mathrm{h1}}^{*}=V_{\mathrm{h1}}+V_{\mathrm{h2}}, \tag{64}$$

$$\mathrm{PH}_1^{*}=\mathrm{PH}_1+\frac{R_{\mathrm{h1}}^2}{R_{\mathrm{h2}}^2}\mathrm{PH}_2. \tag{65}$$

Similarly, more than one horizontal cell network can be added to the model.

4 Discussion

In a continuous two-sheet analytical model of the outer retina, we derived the feedback loop gain that gives the fastest adaptation to light onset and the highest spatial resolution. Starting from the known structure of the outer retina, the model relates feedback loop gains to the space and time constants of photoreceptors and horizontal cells. This is novel and important because it is the first analytical study that derives optimal spatio-temporal dynamic properties of the response from the retinal structure. It is general because it is applicable to the outer retina of all vertebrates.

The model predicts that the outer retina acts as a band-pass filter, removing low and high spatial and temporal frequencies and thus efficiently transmitting changes in local contrast. The spatio-temporal low-pass filter is determined by the spatial and temporal constants of the photoreceptors, while the high-pass filter is formed by negative feedback from horizontal cells. The low-pass filter serves to reduce intrinsic noise of photoreceptors (Lamb and Simon 1976; Smith 1995). In our model, space and time constants are fixed parameters, and are not subject to adjustment to accommodate low contrast light stimuli. Conversely, the negative feedback from horizontal cells to photoreceptors, which forms the high-pass filter and removes the background response, is considered a free parameter to be optimized.

To maximize the temporal contrast resolution, we used both natural stimuli (full-field light onset resulting from large saccade over a light edge) and a full-field temporal sine wave flicker. Maximizing the slew rate in response to full-field light onset and maximizing the product of amplitude and temporal frequency in response to full-field flicker produced the same relationship between the time constants and the optimized feedback gains (23). In order to maximize the spatial contrast resolution, we also used both natural stimuli (a light line onset resulting from a small saccade over a light edge) and a modulated sine grating. Similarly, minimizing the spatial extent of the feedback signal in response to the light line onset and the product of amplitude and spatial frequency in response to a modulated sine grating produced the same relationship between the space constants and the optimized feedback gains (33). Thus, regardless of the definition of the contrast resolution, using either a spatio-temporal impulse response or a transfer function, we obtained the same optimal relationship (Eqs. 23, 33). This optimal relationship between feedback gain and spatial and time constants set the highest spatial and temporal contrast resolution. The high feedback loop gain allows horizontal cells to provide spatially restricted and fast feedback to photoreceptors. Thus, the model predicts relatively large space and time constants of horizontal cells on the assumption that the feedback must be local and fast.

The optimal relationship we obtained (Eqs. 23, 33) predicts a correlation between the space and time constants of photoreceptors and horizontal cells (39). A large increase in background light intensity increases the dopamine release by amacrine cells causing a decrease in horizontal cell coupling (Piccolino et al. 1984;Hampson et al. 1994), which decreases the horizontal cell space constant (Eq. 2.2). On the other hand, the increase in light intensity will also decrease the glutamate release from photoreceptors causing a decrease in the horizontal cell membrane conductance, which would tend to increase the horizontal cell space and time constants (Eqs. 2.2, 2.4). Such a correlated decrease in horizontal cell coupling and membrane conductances might tend to preserve the horizontal cell space constant. However, with all other parameters constant, a decrease in horizontal cell coupling will decrease the feedback loop gain required for the highest spatial contrast resolution. In this case the model results predict that there should be a concomitant decrease in photoreceptor coupling and membrane conductances in order to preserve the optimal relationships between time constants, space constants, and gains (23, 33) to maximize the contrast resolution.

The need to perform adaptation over both small and large signals requires negative feedback, which generates a calcium transient (Fig. 3). The calcium transient in photoreceptors results in a transient glutamate release and subsequent horizontal cell depolarization. The higher the calcium transient, the larger the response of horizontal cells, and the larger the feedback signal will be. Further, the horizontal cell depolarization is followed by a calcium transient in horizontal cells that is thought to regulate synaptic plasticity in the photoreceptor-horizontal cell synapse (Huang et al. 2006). Thus, the calcium transient in photoreceptors is a physiologically relevant parameter for maximizing the outer retina's contrast resolution. The responses to a dark stimulus will have the opposite polarity. The largest calcium transient in response to a light offset occurs at the very beginning of the stimulus, when the suppression from horizontal cells has not been developed yet (Fig. 3). Therefore, the negative feedback from horizontal cells does not change the maximal calcium transient in response to a dark stimulus.

The major limiting assumption of the model is that signal processing in the outer segments and ribbon synapse is linear and stationary. This is commonly termed "small signal analysis" because a small signal does not perturb the steady state conditions much in a dynamic system. The alternative is termed "large signal analysis" because it assumes a signal large enough to interact with the static and dynamic non-linearities (Van Hateren 2005; Van Hateren and Snippe 2007; Van Hateren 2007). Another assumption is that the photo-pigment isomerization

induces a short impulse current in the photoreceptor terminal. In the real retina, this current has a longer duration, ~20ms (Fig. 9 in Friedburg et al. 2004), which adds a lowpass temporal filter between visual stimulus and the photoreceptor terminal. Incorporating this low-pass filter in the model would have a similar effect as an increase in the photoreceptor time constant T_p. This would reduce the optimal feedback loop gain (Eq. 23) originally calculated using T_p as the ratio of membrane capacitance to membrane conductance. We further assumed that the characteristic delay of synaptic transmission (~1 ms, see Fig. 2 in Rabl et al. 2006) is much less than the time constants of photoreceptors and horizontal cells. Because the value of T_p is 5 ms (Smith and Lamb 1997; Nikonov et al. 2006), incorporating this extra 1 ms delay would only slightly change the frequency of oscillations at high feedback loop gains (Eq. 24). However, these two extensions of the model would not change the conclusions.

The model assumes that synaptic input to horizontal cell is achromatic, i.e., horizontal cells collect input from all cones regardless of spectral sensitivity. Horizontal cells are thought to feed back to every cone from which they receive input (Wässle et al. 1978; Kamermans et al. 1991), and this is the case we modeled. Apart from humans and a handful of new-world primates, mammals have two cone types: short wavelength sensitive “blue” cones, and long-wavelength sensitive “green” cones, which comprise the vast majority (Yin et al. 2006). The cones provide indiscriminant inputs to two types of horizontal cells (*A-type* and *B-type*), which, therefore, are achromatic (Wässle et al. 1978). Even in trichromatic primates, inputs to the horizontal cells are achromatic (Dacey 1999; Packer and Dacey 2002). Further, all but one of the bipolar cell types are achromatic (MacNeil and Gaul 2008; Wässle et al. 2009). Our analysis is targeted towards such simpler achromatic systems, and the results may not be applicable to more complex systems, such as the cold-blooded vertebrates, that express spectrally selective horizontal cells (Twig et al. 2003). However, our results will be directly applicable to horizontal cells and most bipolar cells in mammals. Finally, most ganglion and amacrine cell types are achromatic in mammalian retinas (Yin et al. 2006, 2009), and therefore the results are broadly applicable to the vast majority of these retinas.

The model describes the response to white images, to which all cone photoreceptors have similar sensitivities. However, the model holds for chromatic images as well. The response of a photoreceptor layer to a chromatic light is equivalent to that of a white light passed through a neutral density filter with a dot of transparency at each photoreceptor location that is proportional to the photoreceptor spectral sensitivity. In terms of the frequency response, such a neutral density mask would add high-frequency spatial contrast. The model predicts that the temporal frequency response to a red, green or blue stimulus will be low-passed rather than band-passed (Fig. 10), as shown in the literature (Dobkins et al. 1999), and the low spatial frequency response will be significantly increased (i.e., flattened, Kelly 1973). On the other hand, the feedback loop gain cannot follow fast changes at a local point of any image, and should be tuned for space- and time-averages that are white. Therefore, while the response to a chromatic stimulus depends on a specific cone mosaic unique for each given retina (Hofer et al. 2005), the optimal solution (Eqs. 23, 33) does not.

In a similar way the model can be extended from an achromatic horizontal cell network to color opponent networks. Dependence of the feedforward gain on spectral sensitivity of a photoreceptor is a substrate for color-opponency in horizontal cell networks of some vertebrates (Kamermans et al. 1991). The relative gains from a photoreceptor to each horizontal cell network could reflect the spectral sensitivity of that network. However, the model predicts that the weighted sum of a photoreceptor’s feedforward gains should be the same for all photoreceptors (Eq. 65). Thus, several horizontal cell networks, feeding back to a photoreceptor at the loop gain matched to the network space constant, would affect the glutamate release the same way as a single network. Therefore the basic design principles of the outer retina that we have developed here should be conserved throughout all vertebrates.

The model provides some intuition about the role of negative feedback at the cone synapse (Fig. 3a). A light onset can be considered as a change in contrast, or over longer duration and of sufficient spatial extent, as a change in the background light intensity. Multiple small light onsets result in a big increase in background level, which in large signal analysis would hyperpolarize the cone terminal and shift the operating point of the photoreceptor calcium channels. In the absence of feedback, this hyperpolarization would tend to clip the glutamate release for bright light. However, with feedback included, it would oppose the original shift in the operating point (Smith 1995;Van Hateren 2007), thus preserving gain and expanding dynamic range of the synapse. So long as the relationships between spatial constants, temporal constants and synaptic gains are observed over the whole range of light intensity, a large signal analysis can be built upon our model by small increments of background light. As mentioned above in Sect. 3, this would represent adaptation in a general sense to large steps in light intensity. This type of light adaptation over large spatial extent represents a compromise where a reduction in accuracy in the horizontal cell local feedback to individual cones is balanced by the advantage of collecting from a larger pool of cones to get a better average signal (Srinivasan et al. 1982).

One consequence of negative feedback is reduction of gain. Therefore, theoretically, without negative feedback the outer retina could transmit a light contrast via GABA-ergic signaling from horizontal cells to bipolar cells (Vardi et al. 2000; Duebel et al. 2006) with higher gain. However, negative feedback has two benefits: (i) the feedback suppresses glutamate release from photoreceptors, enhancing the stability of operating point and dynamic range of the synapse, (ii) the feedback induces calcium transients in response to photopigment isomerizations to tune the synaptic gains thus maintaining the strength of the synapse in the long-term (Huang et al. 2006). On the other hand, with feedback too fast or too strong the glutamate release will have low sensitivity to a light contrast but high temporal resolution. The feedback loop gain at high temporal frequencies must be less than one to maintain outer retina stability (Fig. 4b). In this study, we showed that the negative feedback gain should be ~0.5 to equalize magnitudes of photoreceptor and horizontal cell responses. This minimizes non-linearities that could occur from clipping and saturation. Overall, the model shows the conditions which optimize feedback gains simultaneously for maximum sensitivity, fastest adaptation and highest resolution.

Although the calcium channel and voltage feedback evoke the same magnitude of calcium transient in response to full-field light onset (undershoot in Fig. 8a), a comparison between the two mechanisms of negative feedback reveals some advantages of the feedback to calcium channel conductance over the voltage feedback: (i) calcium channel feedback is twice as fast and gives higher spatial resolution because it does not interact with photoreceptor membrane capacitance and coupling (Fig. 7a, Fig. 8a); (ii) because of its speed, calcium channel feedback does not cause oscillations (Fig. 4a); (iii) because of its higher spatial resolution, calcium channel feedback generates a larger local calcium transient. Even though the voltage feedback gives step responses twice as high because of the larger space and time constants (Fig. 7b, Fig. 8b), the involvement of photoreceptor membrane capacitance in the voltage feedback results in oscillations at high loop gains (Fig. 4b, Fig. 6b). In order to avoid the oscillations, the feedback must be maintained at a low gain, which will reduce the effectiveness of the surround, but in this case the feedforward surround mechanism might suffice to enhance adaptation and responses to contrast.

Several possible mechanisms for feedback have been described in the literature (Kamermans and Spekreijse 1999). Among the mechanisms for voltage-independent calcium channel feedback, our model is compatible with pH-mediated feedback (Hirasawa and Kaneko 2003; Vessey et al. 2005), ephaptic feedback (Kamermans et al. 2001a,b), $GABA_B$ receptor mediated feedback (Nelson et al. 1990), and adenosine-mediated (Stella et al. 2003, 2007). Among the

voltage feedback mechanisms, our model is compatible with $GABA_A$ receptor mediated feedback (Tatsukawa et al. 2005; Wu 1992).

In real retinas, the response to a full-field light is larger and more transient than the response to a small spot (Kuffler 1953; Ratliff et al. 1967; Foerster et al. 1977; Detwiler et al. 1980). The classic difference of Gaussians receptive field model requires a dependence of the center and surround Gaussian amplitude and radii on the stimulus temporal frequency to fit with experimental data (Frishman et al. 1987), leaving open the question about the mechanism of such dependence. Our model generates a center–surround receptive field, both in spatial and temporal domains, and predicts the large response to full-field light onset and full-field light flicker observed in the real retina, without a dependence of model parameters on stimulus dimensions (Fig. 9, Fig. 10).

Acknowledgments

Authors are grateful to Patrick Roberts, Victor Gurfinkel, and Orin Packer for their valuable comments. The study was supported by NEI grants EY017095 and EY016607.

References

Atick JJ, Redlich AN. Towards a theory of early visual processing. Neural Comp 1990;2:308–320.

Babai N, Thoreson WB. Horizontal cell feedback regulates calcium currents and intracellular calcium levels in rod photoreceptors of salamander and mouse retina. J Physiol 2009;587(10):2353–2364. [PubMed: 19332495]

Barlow HB. Summation and inhibition in the frog's retina. J Physiol 1953;119:69–88. [PubMed: 13035718]

Barlow, HB. Three points about lateral inhibition. In: Rosenblith, WA., editor. Sensory communication. Cambridge: M.I.T. Press; 1961. p. 782-786.

Boahen, KA. CNS Memo CNS-TR-91-06. Pasadena, CA: California Institute of Technology; 1991. Spatio-temporal sensitivity of the retina: a physical model. 91125 http://hebb.mit.edu/courses/9.641/2002/readings/Boahen91.pdf

Borghuis BG, Sterling P, Smith RG. Loss of sensitivity in an analog neural circuit. J Neurosci 2009;29 (10):3045–3058. [PubMed: 19279241]

Byzov AL. Interaction between the horizontal cells of the turtle retina. Neirofiziologiia 1975;7(3):279–286. [PubMed: 1161107]

Campbell FW, Green DG. Optical and retinal factors affecting visual resolution. J Physiol 1965;181(3): 576–593. [PubMed: 5880378]

Copenhagen DR, Hemila S, Reuter T. Signal transmission through the dark-adapted retina of the toad (Bufo marinus). J Gen Physiol 1990;95:717–732. [PubMed: 2110968]

Copenhagen DR, Owen WG. Coupling between rod photoreceptors in a vertebrate retina. Nature 1976;260:57–59. [PubMed: 1264196]

Dacey DM. Primate retina: cell types, circuits and color opponency. Prog Retin Eye Res 1999;18(6):737–763. [PubMed: 10530750]

Dawis S, Shapley R, Kaplan E, Tranchina D. The receptive field organization of X-cells in the cat: spatiotemporal coupling and asymmetry. Vision Res 1984;24(6):549–564. [PubMed: 6740975]

Detwiler PB, Hodgkin AL. Electrical coupling between cones in turtle retina. J Physiol 1979;291:75–100. [PubMed: 225478]

Detwiler PB, Hodgkin AL, McNaughton PA. Temporal and spatial characteristics of the voltage response of rods in the retina of the snapping turtle. J Physiol 1980;300:213–250. [PubMed: 7381784]

DeVries SH, Qi X, Smith R, Makous W, Sterling P. Electrical coupling between mammalian cones. Curr Biol 2002;12:1900–1907. [PubMed: 12445382]

Dobkins KR, Anderson CM, Lia B. Infant temporal contrast sensitivity functions (tCSFs) mature earlier for luminance than for chromatic stimuli: evidence for precocious magnocellular development? Vision Res 1999;39(19):3223–3239. [PubMed: 10615492]

Duebel J, Haverkamp S, Schleich W, Feng G, Augustine GJ, Kuner T, Euler T. Two-photon imaging reveals somatodendritic chloride gradient in retinal ON-type bipolar cells expressing the biosensor Clomeleon. Neuron 2006;49(1):81–94. [PubMed: 16387641]

Enroth-Cugell C, Robson JG. The contrast sensitivity of retinal ganglion cells of the cat. J Physiol 1966;187(3):517–552. [PubMed: 16783910]

Fesenko EE, Kolesnikov SS, Lyubarsky AL. Induction by cyclic GMP of cationic conductance in plasma membrane of retinal rod outer segment. Nature 1985;313(6000):310–313. [PubMed: 2578616]

Field DJ. Relations between the statistics of natural images and the response properties of cortical cells. J Opt Soc Am 1987;4:2379–2394.

Foerster MH, van de Grind WA, Grusser OJ. The response of cat horizontal cells to flicker stimuli of different area, intensity and frequency. Exp Brain Res 1977;29(3–4):367–385. [PubMed: 913523]

Friedburg C, Allen CP, Mason PJ, Lamb TD. Contribution of cone photoreceptors and post-receptoral mechanisms to the human photopic electroretinogram. J Physiol 2004;556:819–834. [PubMed: 14990682]

Frishman LJ, Freeman AW, Troy JB, Schweitzer-Tong DE, Enroth-Cugell C. Spatiotemporal frequency responses of cat retinal ganglion cells. J Gen Physiol 1987;89(4):599–628. [PubMed: 3585279]

Hampson EC, Weiler R, Vaney DI. pH-gated dopaminergic modulation of horizontal cell gap junctions in mammalian retina. Proc Biol Sci 1994;255(1342):67–72. [PubMed: 8153138]

He S, Levick WR. Spatial-temporal response characteristics of the ON-OFF direction selective ganglion cells in the rabbit retina. Neurosci Lett 2000;285:25–28. [PubMed: 10788699]

Hirasawa H, Kaneko A. pH changes in the invaginating synaptic cleft mediate feedback from horizontal cells to cone photoreceptors by modulating Ca2+ channels. J Gen Physiol 2003;122(6):657–671. [PubMed: 14610018]

Hofer H, Carroll J, Neitz J, Neitz M, Williams DR. Organization of the human trichromatic cone mosaic. J Neurosci 2005;25(42):9669–9679. [PubMed: 16237171]

Hosoi N, Arai I, Tachibana MJ. Group III metabotropic glutamate receptors and exocytosed protons inhibit L-type calcium currents in cones but not in rods. Neuroscience 2005;25(16):4062–4072. [PubMed: 15843608]

Huang SY, Hu JF, Gong HQ, Liang PJ. Postsynaptic calcium pathway contributes to synaptic plasticity between retinal cones and luminosity-type horizontal cells. Acta Physiol Sin 2006;58(5):407–414.

Ichinose T, Lukasiewicz PD. Inner and outer retinal pathways both contribute to surround inhibition of salamander ganglion cells. J Physiol 2005;565(2):517–535. [PubMed: 15760938]

Kamermans M, Fahrenfort I, Schultz K, Janssen-Bienhold U, Sjoerdsma T, Weiler R. Hemichannel-mediated inhibition in the outer retina. Science 2001a;292(5519):1178–1180. [PubMed: 11349152]

Kamermans M, Kraaij D, Spekreijse H. The dynamic characteristics of the feedback signal from horizontal cells to cones in the goldfish retina. J Physiol 2001b;534(2):489–500. [PubMed: 11454966]

Kamermans M, Spekreijse H. The feedback pathway from horizontal cells to cones. A mini review with a look ahead. Vision Res 1999;39(15):2449–2468. [PubMed: 10396615]

Kamermans M, van Dijk BW, Spekreijse H. Color opponency in cone-driven horizontal cells in carp retina. Aspecific pathways between cones and horizontal cells. J Gen Physiol 1991;97(4):819–843. [PubMed: 1711573]

Kamermans M, Werblin F. GABA-mediated positive autofeed-back loop controls horizontal cell kinetics in tiger salamander retina. J Neurosci 1992;12(7):2451–2463. [PubMed: 1351934]

Kaneko A. Electrical connexions between horizontal cells in the dogfish retina. J Physiol 1971;213(1): 95–105. [PubMed: 5575346]

Kaneko A, Shimazaki H. Synaptic transmission from photoreceptors to bipolar and horizontal cells in the carp retina. Cold Spring Harb Symp Quant Biol 1976;40:537–546. [PubMed: 7385]

Kelly DH. Theory of flicker and transient responses: II. Count-erphase gratings. J Opt Soc Am 1971;61 (5):632–640. [PubMed: 4323629]

Kelly DH. Lateral inhibition in human colour mechanisms. J Physiol 1973;228(1):55–72. [PubMed: 4686025]

Kuffler SW. Discharge patterns and functional organization of mammalian retina. J Neurophysiol 1953;16(1):37–68. [PubMed: 13035466]

Lamb TD, Simon EJ. The relation between intercellular coupling and electrical noise in turtle photoreceptors. J Physiol 1976;263(2):257–286. [PubMed: 1018249]

Lankheet MJ, Frens MA, van de Grind WA. Spatial properties of horizontal cell responses in the cat retina. Vision Res 1990;30(9):1257–1275. [PubMed: 2219744]

Lankheet MJ, Rowe MH, VanWezel RJ, van de Grind WA. Spatial and temporal properties of cat horizontal cells after prolonged dark adaptation. Vision Res 1996;36(24):3955–3967. [PubMed: 9068849]

Linsenmeier RA, Frishman LJ, Jakiela HG, Enroth-Cugell C. Receptive field properties of X and Y cells in the cat retina derived from contrast sensitivity measurement. Vision Res 1982;22:1173–1183. [PubMed: 7147728]

MacNeil MA, Gaul PA. Biocytin wide-field bipolar cells in rabbit retina selectively contact blue cones. J Comp Neurol 2008;506(1):6–15. [PubMed: 17990268]

McMahon MJ, Packer OS, Dacey DM. The classical receptive field surround of primate parasol ganglion cells is mediated primarily by a non-GABAergic pathway. J Neurosci 2004;24(15):3736–3745. [PubMed: 15084653]

Michael R, Guevara O, de la Paz M, Alvarez de Toledo J, Barraquer RI. Neural contrast sensitivity calculated from measured total contrast sensitivity and modulation transfer function. Acta Ophthalmol 2009 Nov 1;:1–6. 2009.

Miller RF, Dacheux RF. Intracellular chloride in retinal neurons: measurement and meaning. Vision Res 1983;23(4):399–411. [PubMed: 6880038]

Nelson R, Pflug R, Baer SM. Background-induced flicker enhancement in cat retinal horizontal cells. II. Spatial properties. J Neurophysiol 1990;64(2):326–340. [PubMed: 2213121]

Nikonov SS, Kholodenko R, Lem J, Pugh EN Jr. Physiological features of the S- and M-cone photoreceptors of wild-type mice from single-cell recordings. J Gen Physiol 2006;127(4):359–374. [PubMed: 16567464]

Normann RA, Pochobradský J. Oscillations in rod and horizontal cell membrane potential: evidence for feed-back to rods in the vertebrate retina. J Physiol 1976;261(1):15–29. [PubMed: 825636]

Packer OS, Dacey DM. Receptive field structure of H1 horizontal cells in macaque monkey retina. J Vis 2002;2:272–292. [PubMed: 12678578]

Picaud S, Larsson P, Wellis DP, Lecar H, Werblin F. Cone photoreceptors respond to their own glutamate release in the tiger salamander. Proc Natl Acad Sci USA 1995;92:9417–9421. [PubMed: 7568144]

Piccolino M, Neyton J, Gerschenfeld HM. Decrease of gap junction permeability induced by dopamine and cyclic adenosine 3′:5′-monophosphate in horizontal cells of turtle retina. J Neurosci 1984;4(10): 2477–2488. [PubMed: 6092564]

Poggio T, Torre V, Koch C. Computational vision and regularization theory. Nature 1985;317:314–319. [PubMed: 2413361]

Rabl K, Cadetti L, Thoreson WB. Paired-pulse depression at photoreceptor synapses. J Neurosci 2006;26 (9):2555–2563. [PubMed: 16510733]

Ratliff F, Knight BW, Toyoda J, Hartline HK. Enhancement of flicker by lateral inhibition. Science 1967;158:392–393. [PubMed: 6061895]

Rieke F, Schwartz EA. Asynchronous transmitter release: control of exocytosis and endocytosis at the salamander rod synapse. J Physiol 1996;493:1–8. [PubMed: 8735690]

Rodieck RW. Quantitative analysis of cat retinal ganglion cell response to visual stimuli. Vision Res 1965;5:583–601. [PubMed: 5862581]

Shiells RA, Falk G. Contribution of rod, on-bipolar, and horizontal cell light responses to the ERG of dogfish retina. Vis Neurosci 1999;16(3):503–511. [PubMed: 10349971]

Smith RG. Simulation of anatomically defined local circuit: the cone-horizontal cell network in cat retina. Vis Neurosci 1995;12:545–561. [PubMed: 7654610]

Smith NP, Lamb TD. The a-wave of the human electroretinogram recorded with a minimally invasive technique. Vision Res 1997;37(21):2943–2952. [PubMed: 9425511]

Srinivasan MV, Laughlin SB, Dubs A. Predictive coding: a fresh view of inhibition in the retina. Proc R Soc Lond B Biol Sci 1982;216(1205):427–459. [PubMed: 6129637]

Stella SL Jr, Bryson EJ, Cadetti L, Thoreson WB. Endogenous adenosine reduces glutamatergic output from rods through activation of A2-like adenosine receptors. J Neurophysiol 2003;90(1):165–174. [PubMed: 12843308]

Stella SL Jr, Hu WD, Vila A, Brecha NC. Adenosine inhibits voltage-dependent Ca2+ influx in cone photoreceptor terminals of the tiger salamander retina. J Neurosci Res 2007;85(5):1126–1137. [PubMed: 17304584]

Stockton RA, Slaughter MM. Depolarizing actions of GABA and glycine on amphibian retinal horizontal cells. J Neurophysiol 1991;65(3):680–692. [PubMed: 1646870]

Tachibana M, Kaneko A. L-Glutamate-induced depolarization in solitary photoreceptors: A process that may contribute to the interaction between photoreceptors *in situ*. Proc Nati Acad Sci USA 1988;85:5315–5319.

Tatsukawa T, Hirasawa H, Kaneko A, Kaneda M. GABA-mediated component in the feedback response of turtle retinal cones. Vis Neurosci 2005;22(3):317–324. [PubMed: 16079007]

Thoreson WB, Katalin R, Townes-Anderson E, Heidelberger R. A highly Ca2+-sensitive pool of vesicles contributes to linearity at the rod photoreceptor ribbon synapse. Neuron 2004;42:595–605. [PubMed: 15157421]

Tranchina. “Mathematics in visual neuroscience: the retina” in an introduction to mathematical modeling in physiology, cell biology and immunology. In: Sneyd, J., editor. Proceedings of symposia on pure and applied mathematics; 2002. p. 33-55.

Twig G, Levy H, Perlman I. Color opponency in horizontal cells of the vertebrate retina. Prog Retin Eye Res 2003;22(1):31–68. [PubMed: 12597923]

Van Hateren JH. Spatiotemporal contrast sensitivity of early vision. Vision Res 1993;33(2):257–267. [PubMed: 8447098]

Van Hateren JH. A cellular and molecular model of response kinetics and adaptation in primate cones and horizontal cells. J Vis 2005;5(4):331–347. [PubMed: 15929656]

Van Hateren JH, Lamb TD. The photocurrent response of human cones is fast and monophasic. BMC Neurosci 2006;7:34. [PubMed: 16626487]

Van Hateren JH, Snippe HP. Simulating human cones from mid-mesopic up to high-photopic luminances. J Vis 2007;7(4):1–11. [PubMed: 17461685]

Van Hateren JH. A model of spatiotemporal signal processing by primate cones and horizontal cells. J Vis 2007;7(3):1–19. [PubMed: 17461685]

Vardi N, Zhang LL, Payne JA, Sterling P. Evidence that different cation chloride cotransporters in retinal neurons allow opposite responses to GABA. J Neurosci 2000;20(20):7657–7663. [PubMed: 11027226]

Verweij J, Kamermans M, Spekreijse H. Horizontal cells feed back to cones by shifting the cone calcium-current activation range. Vis Res 1996;36:3943–3953. [PubMed: 9068848]

Vessey JP, Stratis AK, Daniels BA, Da Silva N, Jonz MG, Lalonde MR, Baldridge WH, Barnes S. Proton-mediated feedback inhibition of presynaptic calcium channels at the cone photoreceptor synapse. J Neurosci 2005;25(16):4108–4117. [PubMed: 15843613]

Vigh J, Witkovsky P. Sub-millimolar cobalt selectively inhibits the receptive field surround of retinal neurons. Vis Neurosci 1999;16(1):159–168. [PubMed: 10022487]

Wässle H, Boycott BB, Peichl L. Receptor contacts of horizontal cells in the retina of the domestic cat. Proc R Soc Lond B Biol Sci 1978;203(1152):247–267. [PubMed: 84388]

Wässle H, Puller C, Müller F, Haverkamp S. Cone contacts, mosaics, and territories of bipolar cells in the mouse retina. J Neurosci 2009;29(1):106–117. [PubMed: 19129389]

Wu SM. Input-output relations of the feedback synapse between horizontal cells and cones in the tiger salamander retina. J Neurophysiol 1991;65(5):1197–1206. [PubMed: 1651374]

Wu SM. Feedback connections and operation of the outer plexiform layer of the retina. Curr Opin Neurobiol 1992;2(4):462–468. [PubMed: 1525544]

Yagi T, Funahashi Y, Ariki F. Dynamic model of dual layer neural network for vertebrate retina. Proc Int Joint Conf Neural Netw 1989;1:787–789.

Yagi T, Ohshima S, Funahashi Y. The role of retinal bipolar cell in early vision: an implication with analogue networks and regularization theory. Biol Cybern 1997;77:163–171. [PubMed: 9352630]

Yin L, Smith RG, Sterling P, Brainard DH. Chromatic properties of horizontal and ganglion cell responses follow a dual gradient in cone opsin expression. J Neurosci 2006;26(47):12351–12361. [PubMed: 17122060]

Yin L, Smith RG, Sterling P, Brainard DH. Physiology and morphology of color-opponent ganglion cells in a retina expressing a dual gradient of S and M opsins. J Neurosci 2009;29(9):2706–2724. [PubMed: 19261865]

Fig. 1.
Set of bars with stepwise increase in light intensity from left to right. The boundaries can be easily detected, whereas the difference between light intensities in the middle of adjacent bars cannot

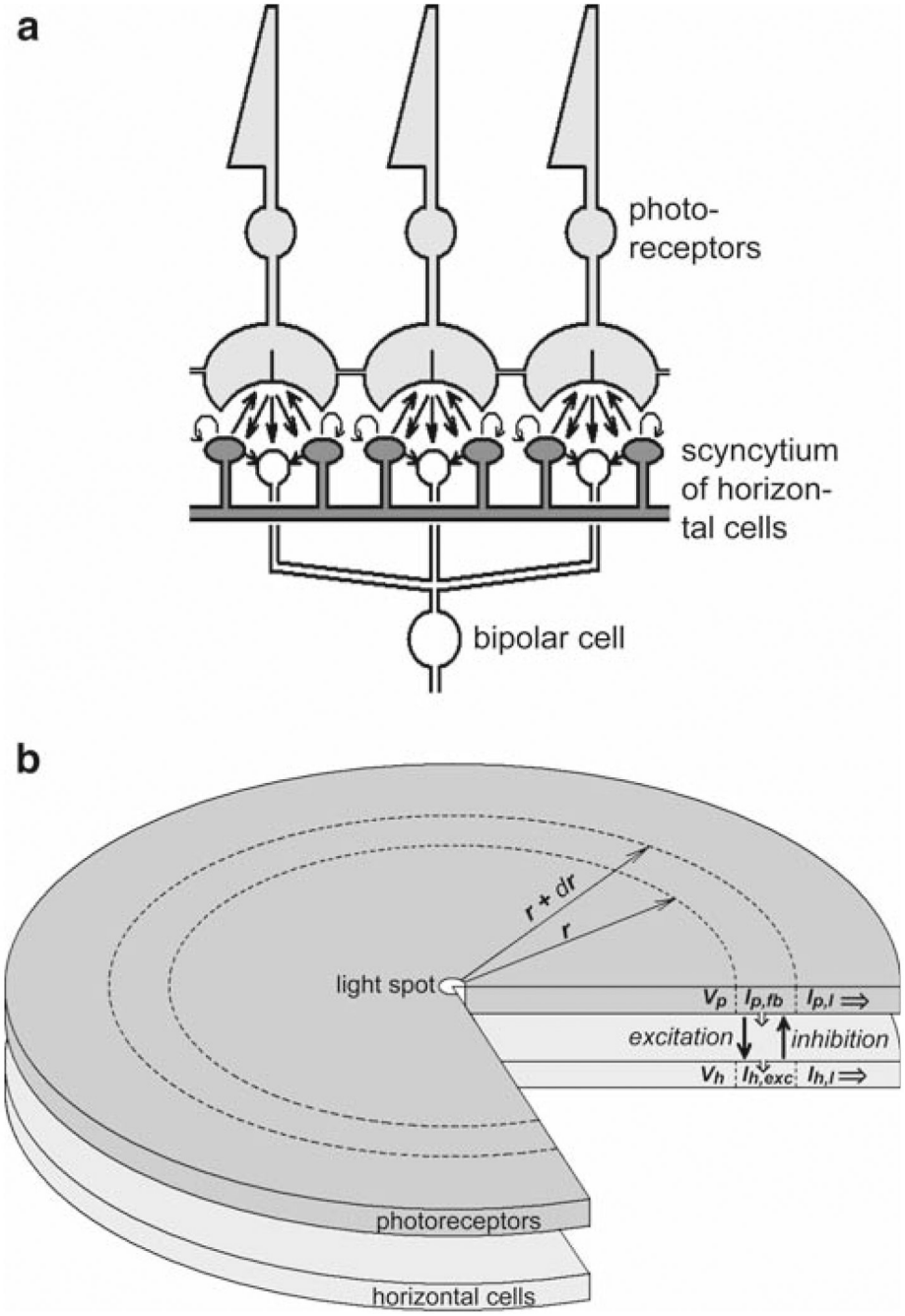

Fig. 2.

a 1D cartoon of the model. Electrically-coupled photoreceptors drive bipolar cells and horizontal cells. Horizontal cells are electrically coupled, inhibit photoreceptors, and drive bipolar cells. **b** 2D continuous model. Hyperpolarization propagates from the light spot across photoreceptor and horizontal cell layers (Eqs. 3.1–3.4). Photoreceptors induce an excitatory current $I_{h,exc}$ in horizontal cells. Horizontal cells induce negative feedback current $I_{p,fb}$ in photoreceptors, and also regulate the voltage-activated calcium conductance in photoreceptors

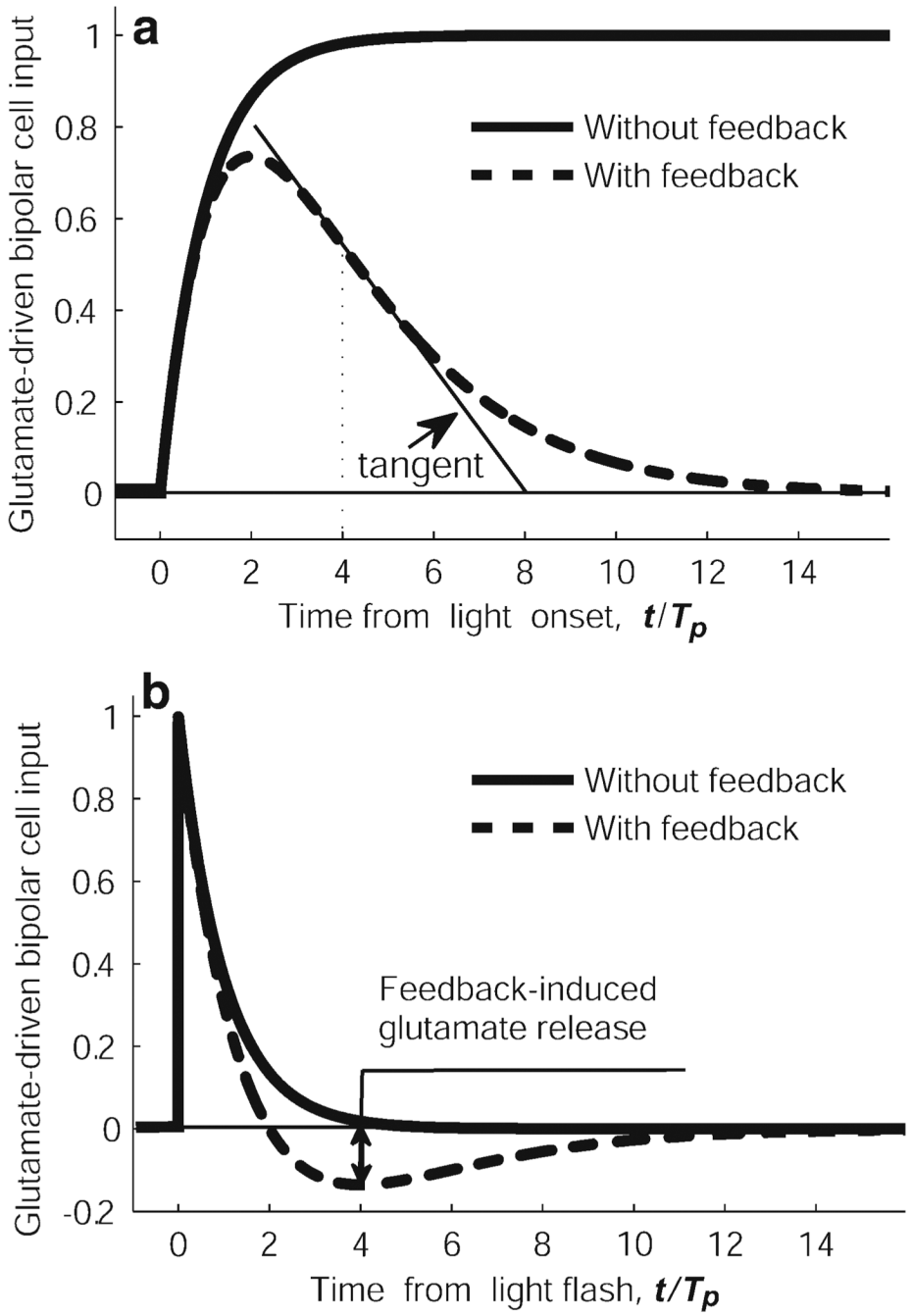

Fig. 3.

Horizontal cell feedback optimized for the fastest adaptation. Normalized responses to a light onset (**a**) and flash (**b**) obtained from Eqs. 18.3 and (17.3), respectively, at HB = 0, HG = 1, HCa = 0, PH · HP = 2.5, and $T_h/T_p \approx 10$ (Smith and Lamb 1997; Nikonov et al. 2006; Kamermans et al. 2001b; Lankheet et al. 1996; Shiells and Falk 1999). Feedback from horizontal cells shortens the duration of glutamate release from the photoreceptors in response to light onset (**a**). The magnitude of the largest slope of the feedback-induced descending part of the step response characterizes the efficiency of the feedback in completing the response and allowing a response to the next stimulus. The largest slope in the step response shown by the tangent line in (**a**) coincides with the largest magnitude of the feedback-induced glutamate

release shown by the undershoot in (**b**) at time $t = 4T_p$. Note that responses are normalized and, therefore, they are identical for bright and dark flashes

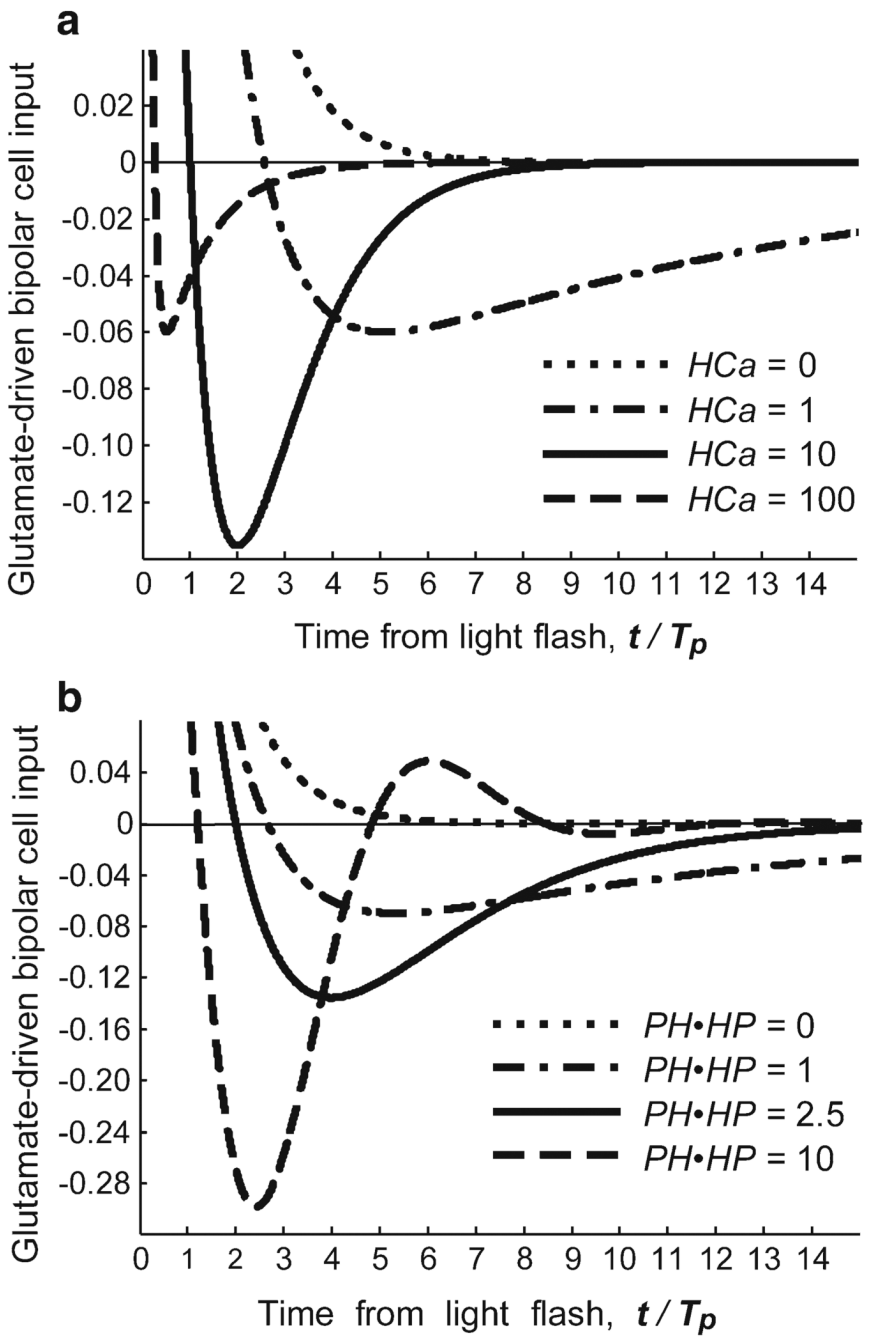

Fig. 4.

The maximum, non-oscillating glutamate release (undershoot) in response to light flash (17.3) is obtained at defined values of the feedback gains: (**a**) Responses with the calcium channel feedback loop gain HCa = 0, 1, 10, 100, and voltage loop gain PH · HP = 0. The T_h/T_p ratio is ~10 (see legend of Fig. 3) giving the optimal loop gain HCa = 10 (Eq. 23). (**b**) Responses with calcium channel feedback loop gain HCa = 0, and voltage loop gain PH · HP = 0, 1, 2.5, 10. The T_h/T_p ratio is set to 10 (from above) giving the optimal voltage loop gain PH·HP = 2.5 (Eq. 23). All traces are normalized to CE · $\Delta V_{p,\mathbf{0}}/T_p$ and converge at point (0, 1). In the absence of the feedback (HCa = 0 or PH · HP = 0) the glutamate transients are never positive (no undershoot). Note that at high loop gain the response has damped oscillations. In order to

prevent the system from oscillating continuously, the feedback loop gain at high temporal frequencies must be lower than unity (Smith 1995)

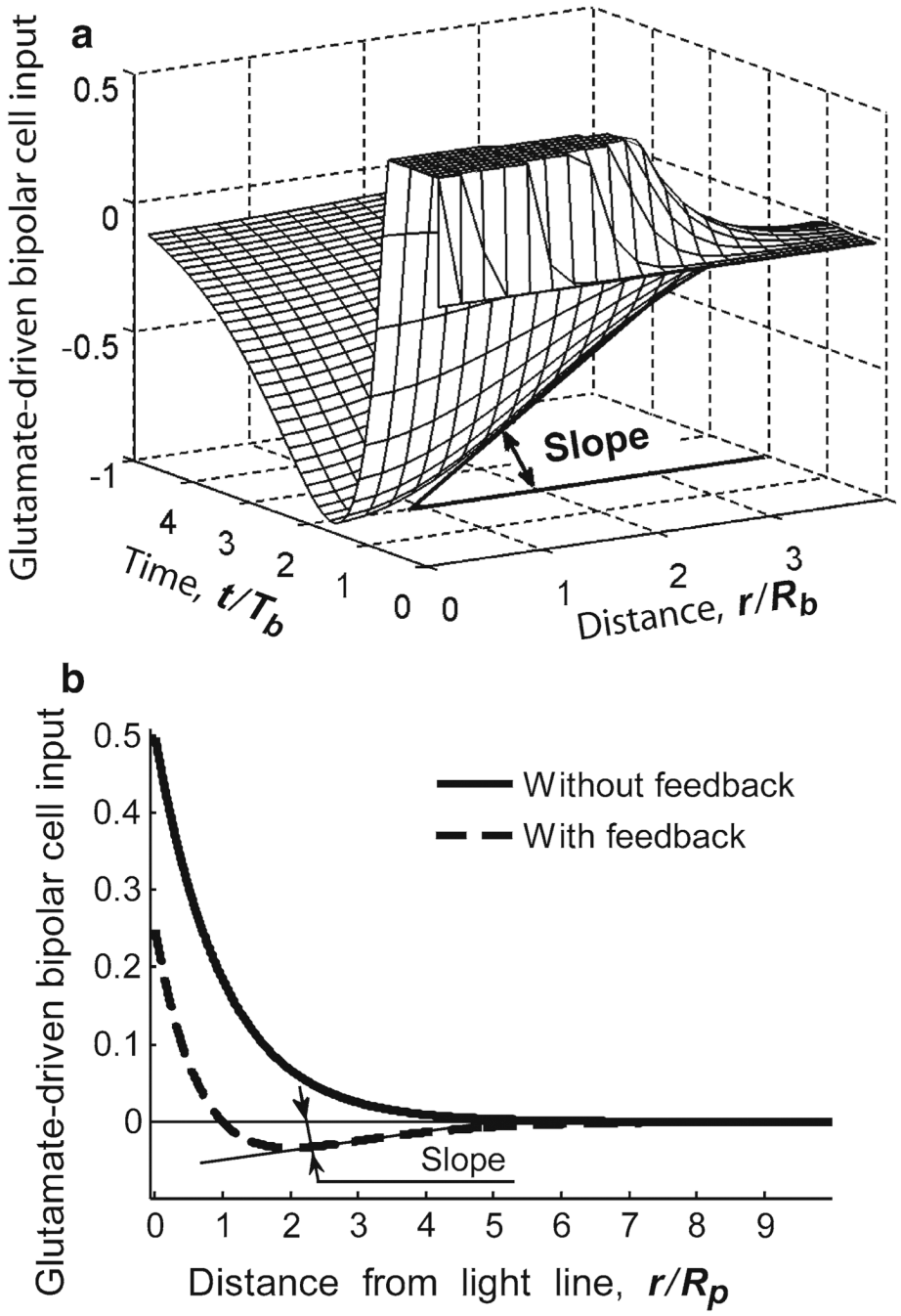

Fig. 5.

Horizontal cell feedback optimized for the highest spatial resolution. **a** The normalized spatio-temporal impulse response of glutamate release obtained from Eqs. 4.1–4.2. The slope determines the spatial spread of the impulse response: the larger the slope the less the spread. The impulse response is truncated at the top. **b** Response to a light line (19.3), normalized to $CE \cdot \Delta V_{p,0}/R_p$, with HB = 0, HG = 1, HCa = 10, and $R_h/R_p \approx 3.2$ (Linsenmeier et al. 1982;Copenhagen et al. 1990). Feedback from horizontal cells generates a negative surround. The greater the slope of the spatial recovery, the narrower the extent of the surround, and the higher the spatial resolution will be. Each point of the spatial impulse response in (**b**) is the time integral of the corresponding spatio-temporal impulse response in (**a**). Equation 23

maximizes the total glutamate transient in response to a light line onset, whereas Eq. 33 maximizes its compactness

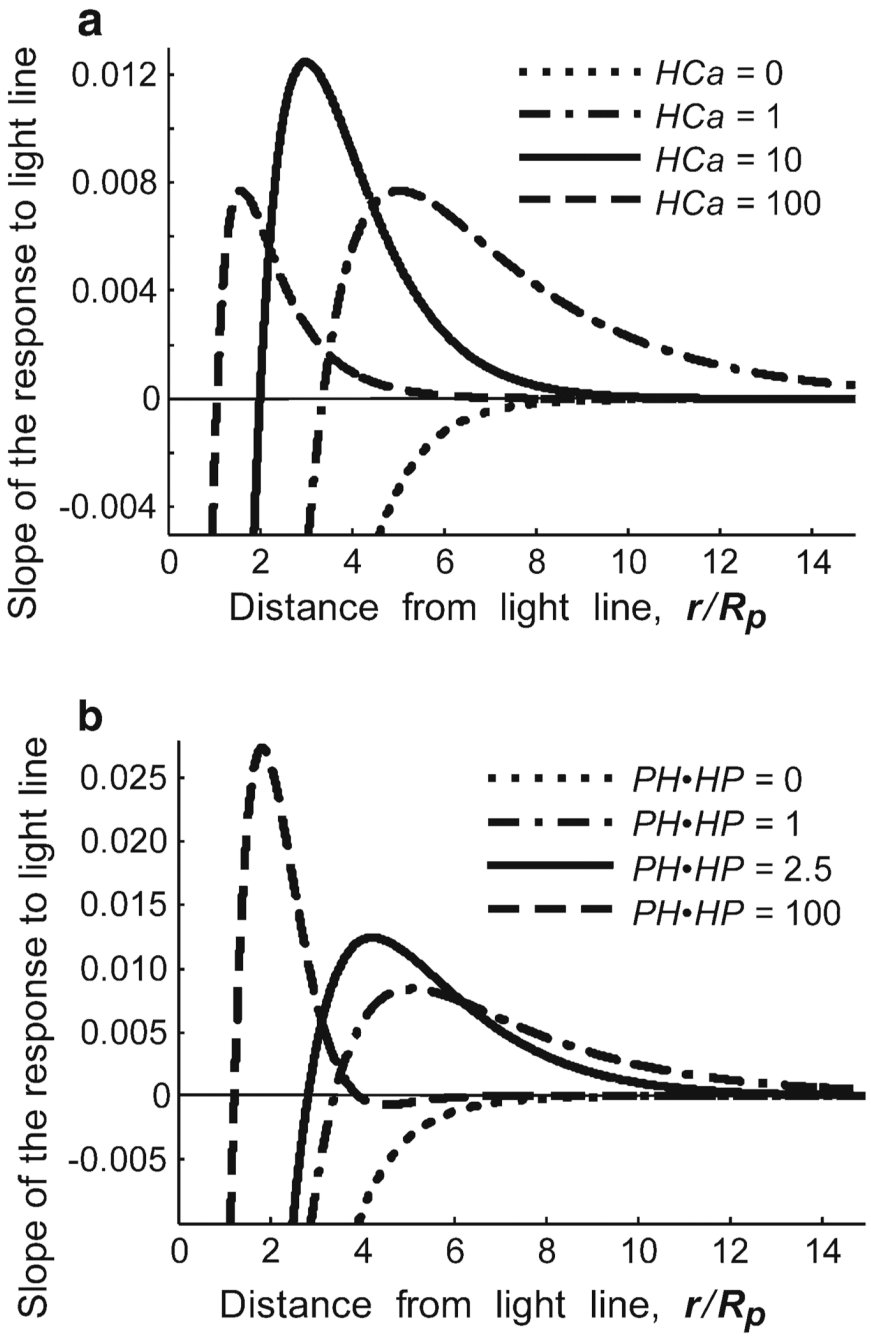

Fig. 6.

The slope in the feedback-induced response to a light line in Fig. 5 is maximized at defined values of the feedback gains. **a** Responses with the calcium channel feedback loop gain HCa = 0, 1, 10, 100, and the voltage loop gain PH · HP = 0. The R_h/R_p ratio is ~3.2 (Linsenmeier et al. 1982;Copenhagen et al. 1990) giving the optimal loop gain HCa ≈ 10 (Eq. 33). **b** Responses with the calcium channel feedback loop gain HCa = 0, and voltage loop gain PH · HP = 0, 1, 2.5, 100. The R_h/R_p ratio is set to ~3.2 (from above) giving the optimal voltage loop gain PH · HP ≈ 2.5 (Eq. 33). At voltage gains higher than optimal, the magnitude of the slope oscillates. All traces are normalized to $\mathrm{CE} \cdot \Delta V_{p,0}/2R_p^2$ and converge at point (0, 1)

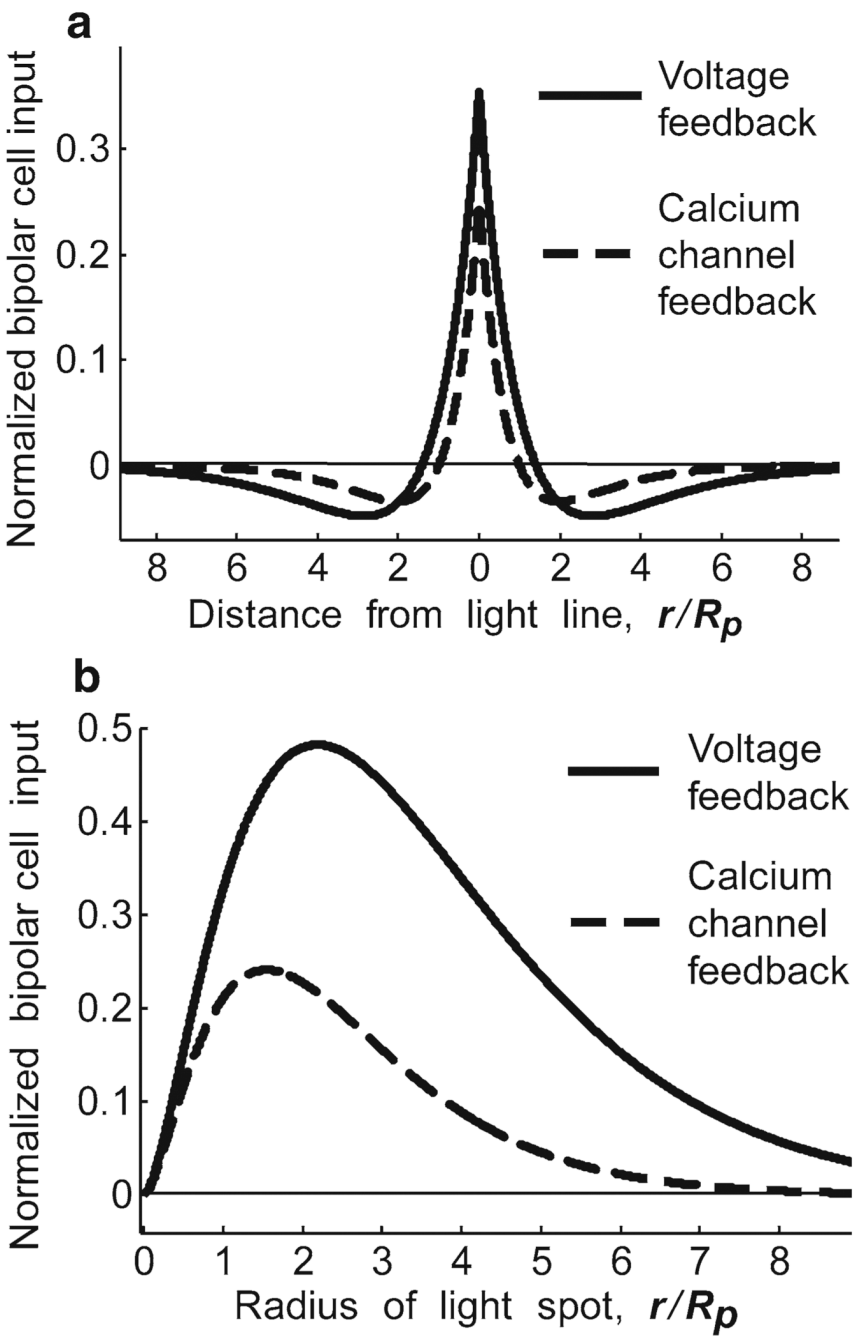

Fig. 7.

Predicted bipolar cell receptive field has center–surround antagonism. (**a**) 1D response (Eq. 50, normalized to CE · $\Delta V_{p,0}/R_p$) consists of center and surround. (**b**) The 2D step response (integral of Eq. 51, normalized to CE · $\Delta V_{p,0}$) reaches its maximum at $r = 1.55\ R_p$ for calcium channel feedback, and at $r = 2.2\ R_p$ for voltage feedback

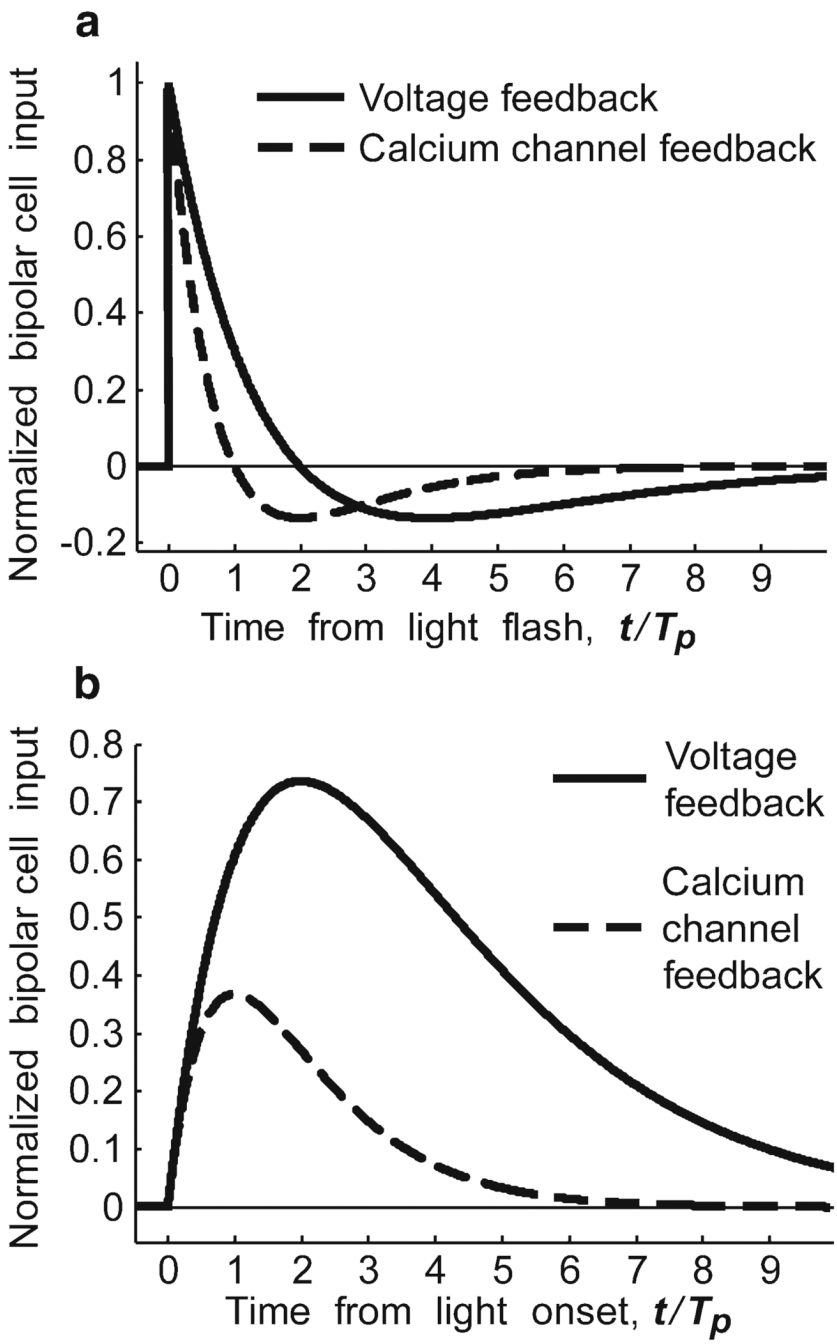

Fig. 8.

a The time-course of the bipolar cell full-field flash-response (Eq. 54, normalized to CE · $\Delta V_{p,0}/T_p$) is biphasic. Note that voltage feedback is twofold slower. **b** The response to full-field light onset, which is the integral of (**a**), reaches its maximum at $t = T_p$ for calcium channel feedback, and at $t = 2T_p$ for voltage feedback

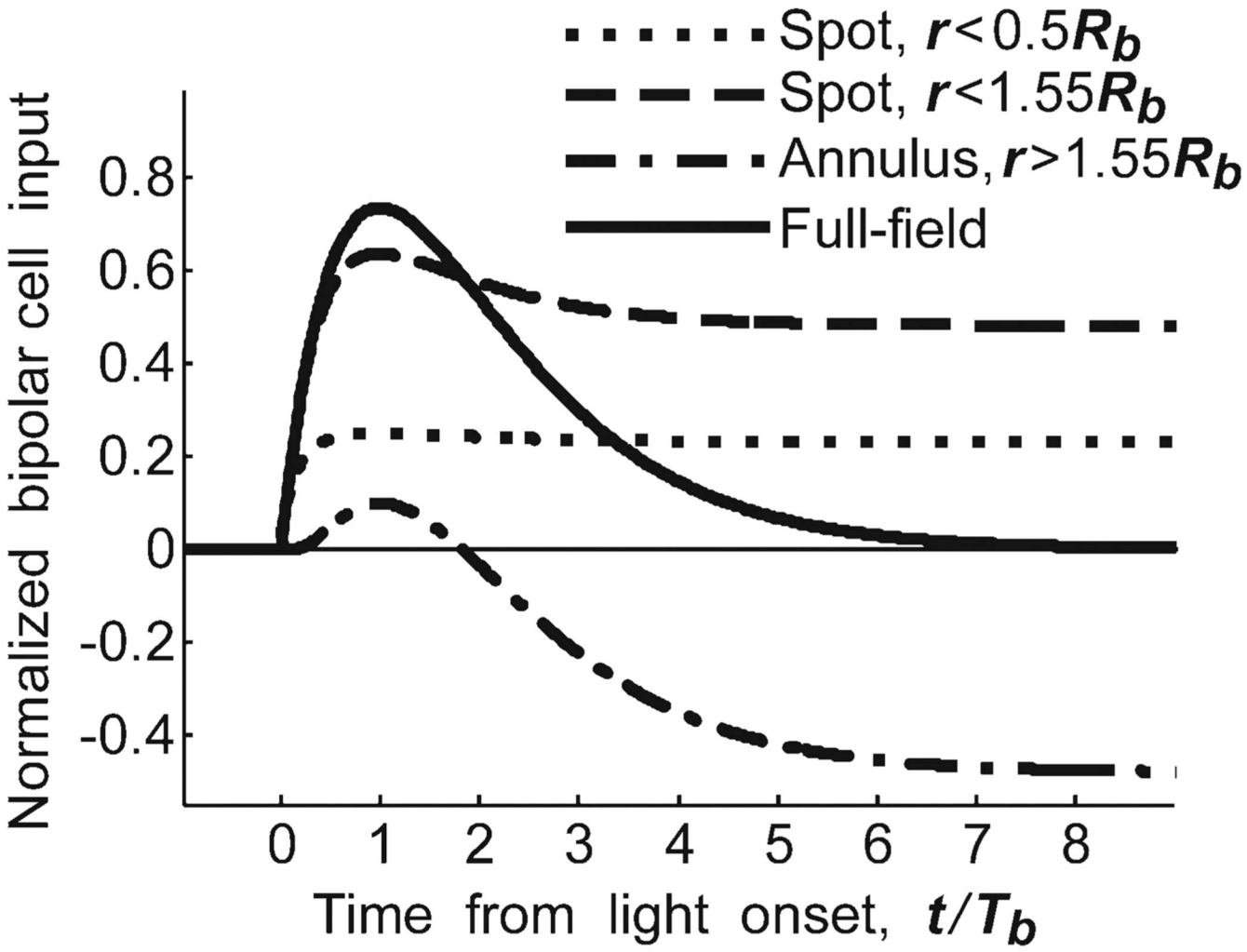

Fig. 9.

Bipolar cell response to the onset of different size spots: *dots*, one third of the diameter of the center receptive field; *dashed*, spot matching the receptive field center; *dash − dots*, annulus matching for the surround; *solid*, full-field spot. The bipolar cell response, normalized to CE $\cdot \Delta V_{p,0}$, is the convolution of the impulse response (Eq. 45 at $T_h/T_p=R_h^2/R_p^2=10$, PH $\cdot$ HP=2.5) and the light spot onset

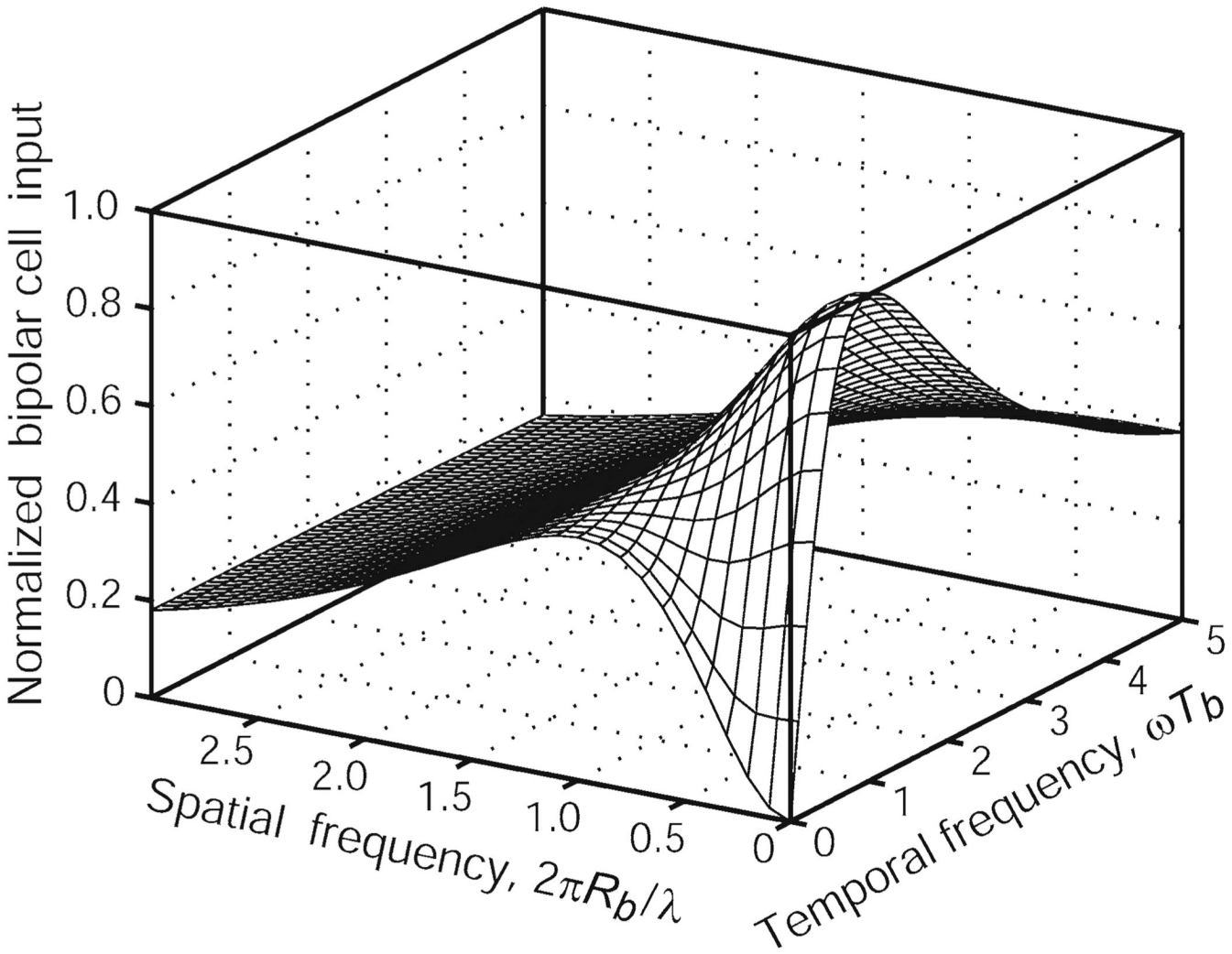

Fig. 10.

Bipolar cell input is spatially and temporally band-passed. The magnitude of the bipolar cell input (56) in response to a moving sine grating is maximal at particular spatial and temporal frequencies (Eq. 57)

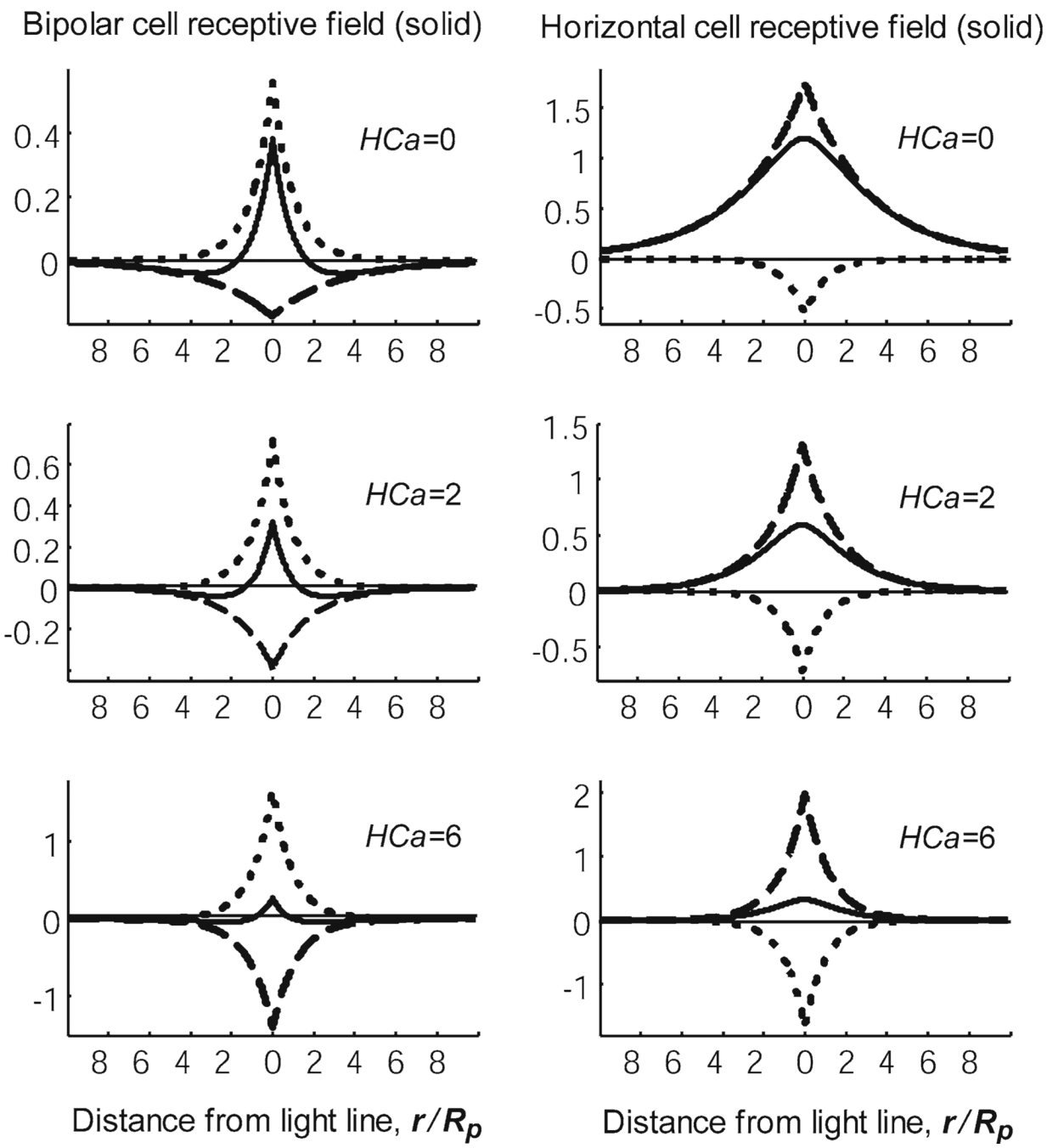

Fig. 11.

Receptive fields of bipolar cell (*left*) and horizontal cell (*right*) are sums of wide (*dashes*) and narrow (*dots*) exponentials (Eqs. 19.1 and 19.3 normalized to CE · $\Delta V_{p,0}/R_p$, with HB = CE/PH, HG = 0, PH = 10, HP = 0, and R_h/R_p = 3.2). The wide exponential (*dashes*) results from signal spread along horizontal cell layer, and the narrow exponential (*dots*) results from signal spread along photoreceptor layer. The width of these exponentials is defined by the corresponding space constants and is modified by the negative feedback. Therefore, fitting single exponential or difference of Gaussians to the receptive fields is inappropriate. The horizontal cell network also feeds forward to bipolar cells, increasing their surround

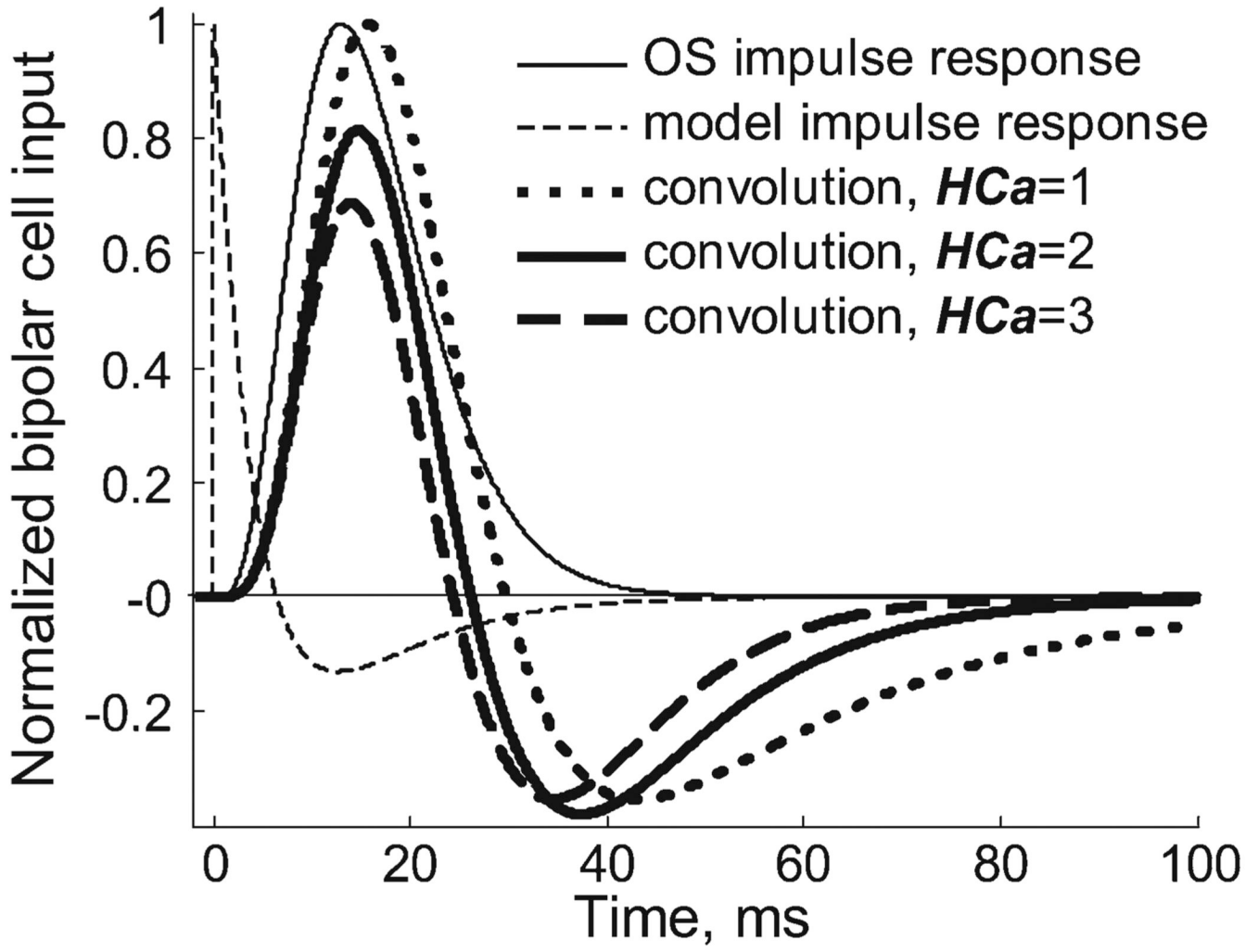

Fig. 12.

Effect of temporal filtering in the outer segments (OS) on the temporal impulse response of bipolar cell input (calcium channel feedback). The OS impulse response at low flash intensity of 22 $T \cdot ds$ (see Fig. 9, Friedburg et al. 2004), has a 10% to 90% rise time of ~7–8 ms (thin solid line). The OS low-pass filter lengthens the impulse response of the bipolar cell input (Eq. 17.3 at HCa = 3, HG = 1, T_p = 5 ms, T_h = 50 ms, thin *dashed line*), decreasing the optimal feedback loop gain from 5 to 2 (*thick solid line*), maximal magnitude of undershoot of the convolved impulse responses), which is roughly equivalent to increasing the cone time constant from 5 ms to 12–13 ms. The OS and the model impulse responses are normalized to their maximal values. The convolutions are normalized together to the maximal value of the convolution at HCa = 1 to compare the magnitudes of the undershoots

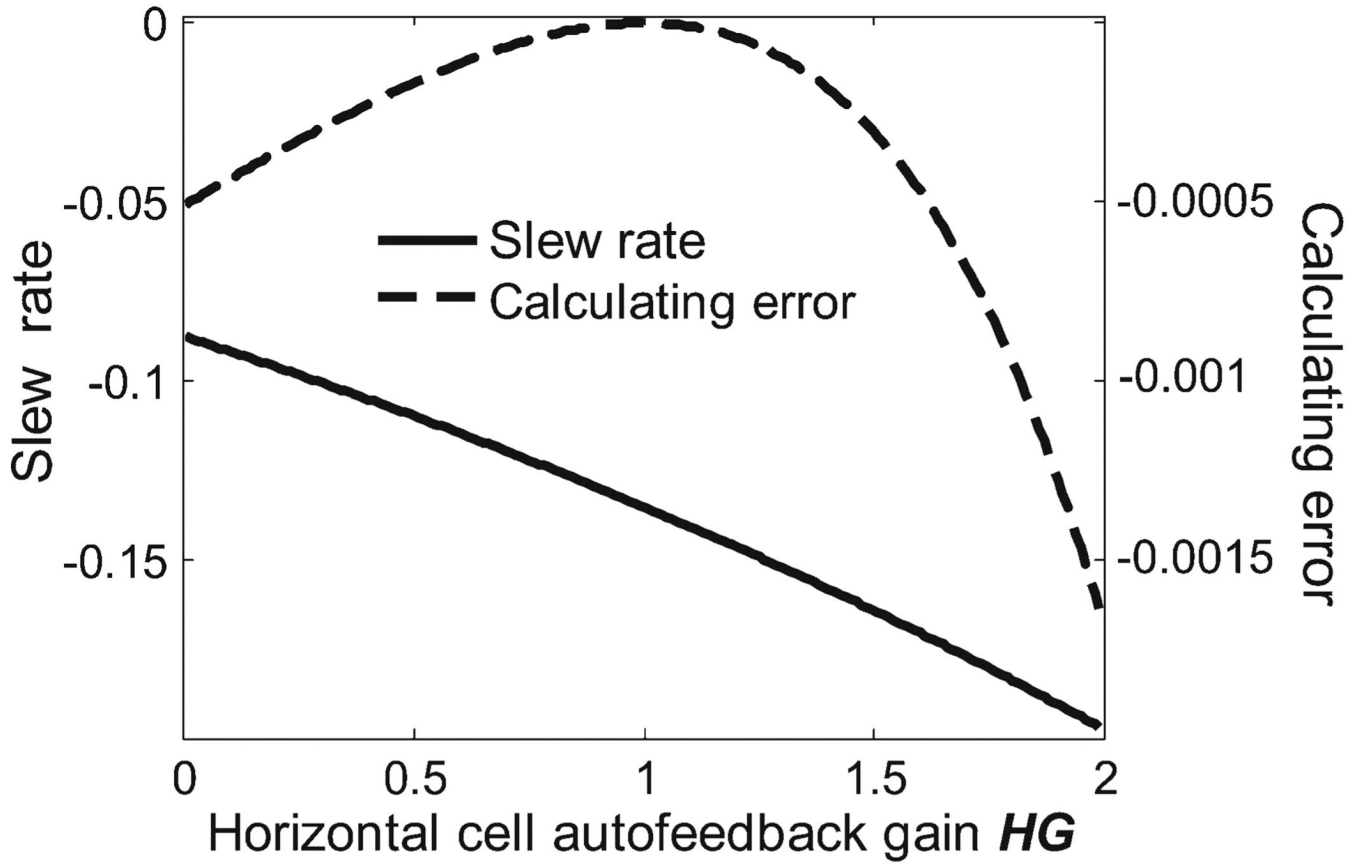

Fig. 13.

Horizontal cell autofeedback increases magnitude of the slew rate (*solid*). The calculating error (*dashed line*), obtained by subtracting the slew rate derived at arbitrary HG (Eq. 17.3) from slew rate derived at HG = 1 (Eq. 54), is less than 1%. Slew rate and calculation error are normalized to CE · $V_{p,0}/T_p$

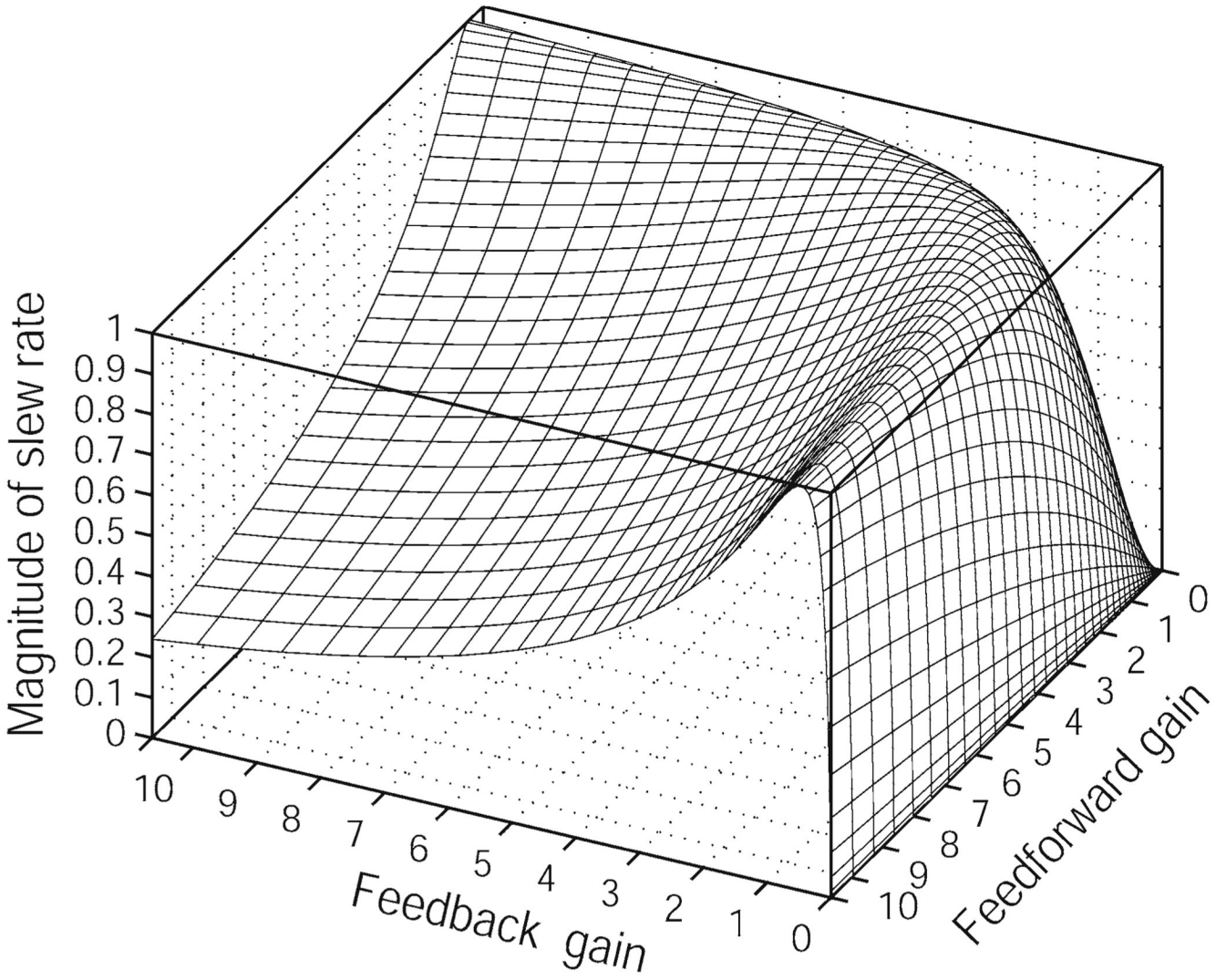

Fig. 14.

The sensitivity of the magnitude of the slew rate on feedforward gain and feedback gain (Eq. 17.3). The magnitude of the slew rate is normalized to its maximum value